eshnr

european society of
head and neck radiology

ESHNR 2016

29th Annual Meeting and Refresher Course

September 22–24, 2016
Leiden/NL

www.eshnr.eu

INDEX

Scientific Information

General Information

Acknowledgements
Photograph: Gerrit Kracht
Map and walks: Laura de Jong

DEAR COLLEAGUES,

On behalf of the European Society of Head and Neck Radiology (ESHNR) it is a great privilege for me to welcome you at the 29th Annual meeting and Refresher Course in Leiden, the Netherlands.

Since 1988 this meeting brings together professionals involved in research and patient care of those afflicted by head and neck diseases. This year, a challenging scientific programme and a comprehensive teaching programme will be offered to discuss state-of-the art imaging and new developments in the field with an emphasis on the technical developments in different imaging techniques. Topics at the cutting edge of development and clinical application will be covered in new horizon sessions, current issues in the field of head and neck radiology will be addressed during scientific sessions and refresher courses. Submitted scientific and educational work will be presented during the scientific programme as well as at the EPOS centre. Also, interactive radiological-anatomical-clinical sessions at the anatomy department and hands-on workshops in ultrasound of the neck have been organized for small groups to consolidate theoretical knowledge and train practical skills. The international faculty comprises head and neck radiologists and experts from allied fields to inspire professional exchange.

During the social events you will be given the opportunity to visit some of the highlights the city of Leiden has to offer: the welcome reception takes place at the City Hall with its monumental renaissaince façade, the gala dinner is held at Hortus Botanicus, the oldest botanical garden in the Netherlands. And I hope you will enjoy exploring the charming historic city centre during a stroll along the canals and picturesque step-gabled houses.

I would like to express my sincere appreciation to the scientific committee, speakers and moderators for kindly accepting to contribute to this meeting.

Wishing you a fruitful meeting and a pleasant stay in Leiden,

Sincerely Yours,

Dr. Berit Verbist
Meeting President ESHNR 2016

PROGRAMME OVERVIEW

Thursday, September 22, 2016

	Room 1 – Burumazaal	Anatomy Lab (Workshops)
08:00		
08:30	Opening Ceremony	
09:00	Scientific Session 1 Infants, toddlers, kids and teens: What's different about them?	Anatomy workshop Spaces of the neck
09:30		
10:00	Coffee Break	
10:30	Short Oral Presentation Session 1 Pre- and postoperative imaging in head and neck oncology	Anatomy workshop Larynx
11:00		
11:30	Industry Sponsored Symposium & Lunch Break	
12:00		
12:30		
13:00	New Horizon Session 1 Elastography: Thyroid and more	
13:30	Scientific Session 2 Thyroid: Cancer vs. incidental finding	
14:00		Anatomy workshop Spaces of the neck
14:30		
15:00	Coffee Break	
15:30	Scientific Session 3 Parathyroid adenomas: Detection & treatment	Anatomy workshop Larynx
16:00		
16:30	Short Oral Presentation Session 2 Tumours and tumefactive lesions	

Friday, September 23, 2016

	Room 1 – Burumazaal	LUMC (Workshops)
08:00	Refresher Course 1 Why are we so fascinated by cranial nerves?	
08:30		
09:00	Scientific Session 4 Skullbase and sinus disease: How to communicate with your clinician?	Ultrasound hands on workshop
09:30		
10:00		
10:30	Coffee Break	
11:00	Short Oral Presentation Session 3 Temporal bone: Lesion characterization and treatment outcome	
11:30		
12:00	Lunch Break	
12:30		
13:00	New Horizon Session 2 – Ultra High Field MRI: Challenges, safety and H&N applications	
13:30	Scientific Session 5 Who is diagnosing hearing loss?	Ultrasound hands on workshop
14:00		
14:30		
15:00	Coffee Break	
15:30	Short Oral Presentation Session 4 Skull base and TMJ: Imaging methods and their yield	
16:00		
16:30	Scientific Session 6 Case-based learning with the expert	
17:00		
17:30		
17:45	General Assembly	

Saturday, September 24, 2016

	Room 1 – Burumazaal
08:00	Refresher Course 2 Morbidity and mortality due to head and neck trauma
08:30	
09:00	Scientific Session 7 CT: Solving clinical problems with new technologies?
09:30	
10:00	
10:30	Coffee Break
11:00	Scientific Session 8 Oncologic imaging: What is the true value of developing imaging techniques?
11:30	
12:00	
12:30	New Horizon Session 3 From photon to proton therapy: Implications for imaging
13:00	Closing Ceremony
	Break
13:30	
	Refresher Course 3 Oral cavity and oropharynx
14:00	
14:30	Refresher Course 4 Salivary gland tumors
15:00	

WORKSHOPS

Workshops will provide interactive demonstrations and opportunities for hands-on experience. It will offer an extremely valuable way to consolidate theoretical knowledge and train practical skills.

The following workshops will be offered:

Thursday, September 22, 2016 – € 50,00

09:00-10:00 and 14:00-15:00
Anatomy workshop – Spaces of the neck

10:40-11:40 and 15:30-16:30
Anatomy workshop – Larynx

These 2 workshops will take place at the anatomy lab. In a joint session an ENT surgeon and a Head & Neck radiologist will demonstrate anatomy and provide clinical and radiological correlation.

Friday, September 23, 2016 – € 75,00

09:00-12:00 and 13:45-16:45
Ultrasound hands on workshop

This hands-on teaching session will guide participants systematically through ultrasound examination of the neck.

For information on availability of places, please visit the registration desk.

PROGRAMME THURSDAY, SEPTEMBER 22, 2016

08:30	**Opening Ceremony**	*B.M. Verbist, Leiden/NL*

08:45–10:15	**SS 1**	**Infants, toddlers, kids and teens: What's different about them?** *Moderators: S. Kösling, Halle a. d. Saale/DE; M. de Win, Amsterdam/NL*
08:45	SS 1.1.	Developmental abnormalities of pharyngeal arches *I. Schmalfuss, Gainesville/US*
09:15	SS 1.2.	Vascular tumors and vascular malformations *M.G. Mack, Munich/DE*
09:45	SS 1.3.	Head and neck oncology in minors *E.E. Deurloo, Amsterdam/NL*

10:15–10:45 Coffee Break

10:45–11:45	**SOPS 1**	**Pre- and postoperative imaging in head and neck oncology** *Moderators: F. Dubrulle, Lille/FR; L. Jacobi-Postma, Maastricht/NL*
10:45	SOPS 1.1.	Radiogenomics in retinoblastoma: Identification of non-invasive MR imaging features as a biomarker for tumor gene-expression profiles in retinoblastoma *R.W. Jansen, Amsterdam/NL*
10:52	SOPS 1.2.	Follow-up of operated cancer of the oral cavity: Don't worry, it's just a PET uptake! *G. Squassina, Brescia/IT*
10:59	SOPS 1.3.	Intravoxel incoherent motion imaging in head and neck cancer: A systematic review *D. Noij, Amsterdam/NL*
11:06	SOPS 1.4.	Do quantitative diffusion weighted MRI parameters reflect human papilloma virus status in oropharyngeal and oral cavity head and neck squamous cell carcinoma? *V. Lenoir, Geneva/CH*
11:13	SOPS 1.5.	The role of diffusion-weighted imaging at high b values in differentiation between benign and malignant cervical lymph nodes *T. Durakoglugil, Rize/TR*
11:20	SOPS 1.6.	Diagnostic accuracy of MRI techniques for treatment response evaluation in patients with head and neck tumours, a systematic review and meta-analysis *A. van der Hoorn, Groningen/NL*
11:27	SOPS 1.7.	MR imaging after nasopharynx endoscopic resection (NER): Normal findings and complications *I. Zorza, Brescia/IT*

11:34	SOPS 1.8.	Adenoid cystic carcinoma of the head and neck region – morphologic characteristics in MRI *S. Greschus, Bonn/DE*
11:37	SOPS 1.9.	SPECT-CT for identification of sentinel lymph nodes in early stage oral cancer *I. den Toom, Utrecht/NL*

POSTER SNAPSHOT

POSTER SNAPSHOT

11:45–13:00 Industry Sponsored Symposium & Lunch Break

13:00–13:30	**NHS 1**	**Elastography: Thyroid and more** *K.S.S. Bhatia, Hong Kong/HK*

13:30–15:00	**SS 2**	**Thyroid: Cancer vs incidental finding** *Moderators: I. Schmalfuss, Gainesville/US; A. van der Lugt, Rotterdam/NL*
13:30	SS 2.1.	Thyroid cancer, facts and figures: An overview *R. Evans, Wales/UK*
13:50	SS 2.2.	Management of the incidental thyroid nodule *R. Rhys, Cardiff/UK*
14:15	SS 2.3.	Panel discussion: Differences in national guidelines *Speakers and Moderators*
14:35	SS 2.4.	Question and answer session: Audience and experts share their views *K.S.S. Bhatia, Hong Kong/HK; J. Kievit, Leiden/NL, Speakers and Moderators*

15:30–16:30	**SS 3**	**Parathyroid adenomas: Detection & treatment** *Moderators: C. Czerny, Vienna/AT; P. de Graaf, Amsterdam/NL*
15:30	SS 3.1.	Clinical aspects of hyperparathyroid disease *J. Kievit, Leiden/NL*
15:40	SS 3.2.	Diagnostic value of US, CT & MRI *P. Richards, London/UK*
16:00	SS 3.3.	Contribution of metabolic imaging *B. de Keizer, Utrecht/NL*
16:20	SS 3.4.	Surgical treatment *J. Kievit, Leiden/NL*

16:30–17:00	**SOPS 2**	**Tumours and tumefactive lesions** *Moderators: H.B. Eggesbo, Oslo/NO; M. Lamers, Groningen/NL*
16:30	SOPS 2.1.	Hypoglossal Canal Lesions: Differentiation of Craniocervical Junction Juxtaarticular Cysts and „Cystic“ Hypoglossal Schwannoma *S. Weindling, Jacksonville/US*
16:37	SOPS 2.2.	Imaging findings in recurrent left cervical swelling syndrome *R. Hermans, Leuven/BE*
16:44	SOPS 2.3.	Eosinophilic Angiocentric Fibrosis (EAF): CT and MRI findings from the largest reported single institution series *S. Jawad, London/UK*
16:51	SOPS 2.4.	High specificity of Intravoxel Incoherent Motion (IVIM) parameter thresholds in differentiating benign and malignant salivary gland tumours *Y.L. Dai, Hong Kong/HK*

PROGRAMME FRIDAY, SEPTEMBER 23, 2016

08:00–09:00	**RC 1**	**Why are we so fascinated by cranial nerves?**
08:00	RC 1.1.	Non-oncologic peripheral nerve palsy: Etiology and imaging findings in benign disorders *A. Borges, Lisbon/PT*
08:20	RC 1.2.	Perineural tumor spread: Common pathways *B.F. Schuknecht, Zurich/CH*
08:40	RC 1.3.	Neural imaging after surgery/radio(chemo)therapy *D. Farina, Brescia/IT*
09:00–10:30	**SS 4**	**Skullbase and sinus disease: How to communicate with your clinician?** *Moderators: S. Robinson, Vienna/AT; S. Steens, Nijmegen/NL*
09:00	SS 4.1.	Anatomical terminology of paranasal sinus and nose *T. Beale, London/UK*
09:30	SS 4.2.	Paranasal and skull base endoscopic surgery: Clinico-radiological session *R. Maroldi, P. Nicolai, Brescia/IT*
10:30–11:00	*Coffee Break*	
11:00–12:00	**SOPS 3**	**Temporal bone: Lesion characterization and treatment outcome** *Moderators: S. Petrovic, Nis/RS; T.A.G.G. Ferreira, Leiden/NL*
11:00	SOPS 3.1.	How to differentiate schwannomas from meningiomas of the IAM on a 3T MRI? Analyze endolymphatic and perilymphatic signal on a high-resolution gradient-echo T2 sequence! *A. Venkatasamy, Strasbourg/FR*
11:07	SOPS 3.2.	Sigmoid sinus diverticulum/dehiscence and dural venous sinus stenosis: Potential aetiologies for pulsatile tinnitus in patients with IIH? *A.L. Carlton Jones, London/UK*
11:14	SOPS 3.3.	Superior semicircular canal dehiscence as a potential aetiology for pulsatile tinnitus in idiopathic intracranial hypertension *M. Eriksen, Stavanger/NO*
11:21	SOPS 3.4.	Malformation of the lateral semicircular canal correlated with data from the audiogram *D. le Foll, Strasbourg/FR*
11:28	SOPS 3.5.	Cochlear aperture development in relation to age *S.E. Sanverdi, Ankara/TR*
11:35	SOPS 3.6.	Perioperative scalar localization and cochlear trauma evaluation using high resolution CBCT and MRI image fusion *S. Peters, Nijmegen/NL*

11:42 SOPS 3.7. Preliminary Outcome of Cochlear Implantation in Children with Hypoplasia of the Cochlear Nerve
A. Giesemann, Hannover/DE

11:49 SOPS 3.8. Visibility of the discomallear ligament on high-resolution computed tomography of the temporal bone
E. Arkink, Leiden/NL

11:52 SOPS 3.9. Holes in the skull – The differential diagnosis of lytic skull lesions
M. Diogo, Lisbon/PT

12:00–13:00 Lunch Break

13:00–13:30 NHS 2 Ultra High Field MRI: Challenges, safety and H&N applications
A.G. Webb, Leiden/NL

13:30–15:00 SS 5 Who is diagnosing hearing loss?
Moderators: B. de Foer, Antwerp/NL; J.-C. de Groot, Groningen/NL

13:30 SS 5.1. Otogenetics: Diagnosing hereditary hearing loss
S. Kant, M. Kriek, Leiden/NL

13:50 SS 5.2. Imaging findings in congenital hearing loss
J.W. Casselman, Bruges/BE

14:30 SS 5.3. Treatment options and postoperative imaging
B.M. Verbist, Leiden/NL

15:00–15:30 Coffee Break

15:30–16:30 SOPS 4 Skull base and TMJ: Imaging methods and their yield
Moderators: D.A. Varoquaux, Marseille/FR; C. Karaman, Aydin/TR

15:30 SOPS 4.1. MR imaging of cranial nerves in the cavernous sinus: Comparison between 3D-VIBE and contrast-enhanced 3D-CISS
M. Ravanelli, Brescia/IT

15:37 SOPS 4.2. Diagnostic efficacy and therapeutic impact of computed tomography in the evaluation of clinically suspected otosclerosis
C. Dudau, London/UK

15:44 SOPS 4.3. Influence of voxel sizes and slice thickness for the assessment of semicircular canals: Comparison of Cone Beam CT and Multislice CT
K. Orhan, Ankara/TR

15:51 SOPS 4.4. MRI of acute mastoiditis: Comparison of temporal bone imaging findings with CECT and with incidental pathology in MRI
R. Saat, Helsinki/FI

15:58 SOPS 4.5. Magnetic resonance imaging of temporomandibular joint dysfunction – correlation with clinical symptoms, age, and gender
J. Avsenik, Ljubljana/SI

16:05 SOPS 4.6. MRI assessment of the temporal layer of bilaminar zone in patients with Temporomandibular joint (TMJ) dysfunction
A. Lo Casto, Palermo/IT

16:12 SOPS 4.7. Assessment of the diagnostic accuracy of contrast-enhanced CT in the detection of salivary gland and ductal calculi compared to non-contrast CT
Y. Purcell, Dublin/IE

16:19 SOPS 4.8. Ultrasonographic Appearances of Parathyroid Gland in Tertiary Hyperparathyroidism
V. Mingkwansook, Pathumthani/TH

POSTER SNAPSHOT

16:22 SOPS 4.9. High resolution ultrasound of the larynx: Imaging technique, normal anatomy and spectrum of disease
S. Jawad, London/UK

POSTER SNAPSHOT

16:30–17:45 SS 6 Case-based learning with the expert
Moderator: F. Pameijer, Utrecht/NL
I. Schmalfuss, Gainesville/US

17:45 ESHNR General Assembly

PROGRAMME SATURDAY, SEPTEMBER 24, 2016

08:00–09:00	**RC 2**	**Morbidity and mortality due to head and neck trauma**
08:00	RC 2.1.	Laryngeal trauma *R. Kohler, Sion/CH*
08:20	RC 2.2.	Trauma of the skull base *E. Loney, Darlington/UK*
08:40	RC 2.3.	Orbital trauma *P. de Graaf, Amsterdam/NL*

09:00–10:30	**SS 7**	**CT: Solving clinical problems with new technologies?** *Moderators: D. Haba, Iasi/RO; M. Palm, Maastricht/NL*
09:00	SS 7.1.	Dual energy CT: Applications in Head and Neck radiology *L. Jacobi-Postma, Maastricht/NL*
09:30	SS 7.2.	CT perfusion: Will it replace MR perfusion? *A. Trojanowska, Lublin/PL*
10:00	SS 7.3.	CBCT: Dental and maxillofacial imaging *R. Saat, Helsiniki/FI*

10:30–11:00 Coffee Break

11:00–12:30	**SS 8**	**Oncologic imaging: What is the true value of developing imaging techniques?** *Moderators: J. Olliff, Birmingham/UK; J.A. Castelijns, Amsterdam/NL*
11:00	SS 8.1.	DWI and DCE MRI *R. Hermans, Leuven/BE*
11:30	SS 8.2.	PET MRI *M. Becker, Geneva/CH*
12:00	SS 8.3.	Sentinel lymph node imaging in the head and neck: Principles and clinical applications *R. de Bree, Amsterdam/NL*

12:30–13:00	**NHS 3**	**From photon to proton therapy: Implications for imaging** *A. Jensen, Bern/CH*

13:00–13:15 Closing Ceremony
B.M. Verbist, Leiden/NL

13:15–13:45 Break

13:45–14:30	**RC 3**	**Oral cavity and oropharynx**
13:45	RC 3.1.	Digital supported interactive learning: Anatomy based approach of spread of diseases: Oral cavity and floor of the mouth *A. van der Gijp, F.A. Pameijer, Utrecht/NL*
14:10	RC 3.2.	The normal and diseased oropharynx *M. Lemmerling, Beervelde/BE*

14:30–15:15	**RC 4**	**Salivary gland tumors**
14:30	RC 4.1.	Neoplasms of the salivary glands *M. de Win, Amsterdam/NL*
15:00	RC 4.2.	Diagnosis and staging of salivary gland tumors *N.J.M. Freling, Amsterdam/NL*

ORAL PRESENTATION ABSTRACTS

SS 1.1.
Developmental abnormalities of pharyngeal arches

I. Schmalfuss, Gainesville/US

Short Summary: The branchial apparatus is composed of arches, pouches and clefts. Each arch is composed of mesoderm that is lined by entoderm and covered by ectoderm. Each of the arches contains a muscular, skeletal, vascular and nerve component leading to a wide range of developmental anomalies:

The 1st branchial arch gives rise to the trigeminal nerve and all muscles supplied by the motoric branch of the mandibular nerve, facial artery, malleus and incus as well as portions of the mandible. The 1st branchial cleft develops into the external auditory canal and auricle while the Eustachian tube, tympanic cavity and mastoid air cells arise from the 1st branchial pouch. Therefore, developmental anomalies of the 1st branchial apparatus manifest with micrognathia, facial clefting, branchial cleft cysts or fistulas, auricular deformity, external auditory canal atresia/stenosis and middle ear abnormalities.

The 2nd branchial arch gives rise to the facial nerve and all muscles supplied by it, stapes, styloid process, stylohoid ligament, external carotid artery and parts of the hyoid bone. The 2nd branchial cleft develops into the cervical sinus of His while the palatine tonsil arises from the 2nd branchial pouch. Developmental anomalies of the 2nd branchial apparatus are most common and primarily manifest with branchial cleft cysts or fistulas that are classified as Bailey type 1 through 4 based on their location and course.

The 3rd branchial arch gives rise to the glossopharyngeal nerve, stylopharyngeus muscle, internal carotid artery and parts of the hyoid bone. The 3rd branchial cleft also develops into the cervical sinus of His while the inferior parathyroid glands, thymus and the pyriform fossa arise from the 3rd branchial pouch. Therefore, developmental anomalies of the 3rd branchial apparatus manifest as branchial cleft cysts or fistulas as well as ectopic parathyroid glands and/or thymus.

The 4th and 5th branchial arches give rise to the vagus nerve, laryngeal cartilages as well as some pharyngeal and laryngeal muscles. The 4th branchial cleft also develops into the cervical sinus of His while the superior parathyroid glands, apex of the piriform sinus and the C cells of the thyroid gland arise from the 4th and 5th branchial pouches. Developmental anomalies of the 4th and 5th branchial apparatus are exceedingly rare and manifest as ectopic parathyroid glands and branchial cleft cysts or fistulas.

Examples of the above listed anomalies will be discussed and illustrated with different imaging modalities during the presentation.

SS 1.2.
Vascular tumors and vascular malformations
M. Mack, Munich/DE

Short Summary: Vascular tumors and malformations can involve all parts of the head and neck in both adults and children. The goal of this presentation is to clarify the nomenclature and to demonstrate the typical imaging appearance. MR imaging is including static and dynamic sequences as well as MR angiography. Dynamic time-resolved contrast enhanced MR angiography provides useful information about the hemodynamics of vascular anomalies and allows differentiation of high-flow and low-flow vascular malformations. Furthermore, MR imaging is useful in assessment of treatment success.

Take Home Points:
1. To differentiate vascular tumors and vascular malformations
2. To understand the use of the different imaging modalities

SS 1.3.
Head and neck oncology in minors
E. Deurloo, Amsterdam/NL

Short Summary: Head and neck masses occur relatively common in pediatric patients. In contrast to adults, the majority of these masses are benign. Head and neck malignancy is less common in children: reported incidence in children under 15 years of age is 1.6 per 100 000. About 12% of all pediatric malignancies occur in the head and neck.

The type of tumor occurring in pediatric patients is strongly correlated with the age of the child. In infants, retinoblastoma, neuroblastoma, germ cell tumors and rhabdomyosarcoma are the most common types. In children 1-5 years of age, retinoblastoma, rhabdomyosarcoma, and lymphoma predominantly occur. In children 6-10 years of age, lymphoma, rhabdomyosarcoma and thyroid cancer are most common. In teenagers, thyroid cancer, lymphoma and nasopharyngeal carcinoma occur. Langerhans cell histiocytosis occurs in all age-groups.

Imaging of (malignant) head and neck tumors in children can be done with ultrasound, CT scan and/or MRI, depending on the symptoms and location of the lesion, and keeping the ALARA-principle in mind (As Low As Reasonably Achievable).

The aim of imaging in pediatric head and neck oncology is to characterize the lesion and make a differential diagnosis, to assess the extent of the lesion, involvement of adjacent structures, and presence of metastases, to guide biopsy and to evaluate response to treatment.

Several tumor types as well as important imaging characteristics which may influence therapy, (e.g. perineural spread, dural involvement and intracranial extension) will be discussed in the presentation.

Take Home Points:
- Malignant head and neck tumors in children are quite rare.
- Tumor types are roughly correlated to the age of the patient.
- It is important to assess the extent of the lesion and involvement of adjacent structures, e.g., nerves and dura.

SOPS 1.1.

Radiogenomics in retinoblastoma: identification of non-invasive MR imaging features as a biomarker for tumor gene-expression profiles in retinoblastoma

R.W. Jansen[1], M. de Jong[1], I.E. Kooi[1], S. Sirin[2], S.L. Göricke[2], H.J. Brisse[3], P. Maeder[4], P. Galluzzi[5], P. van der Valk[1], J. Cloos[1], I. Eekhout[1], H.C.W. de Vet[1], J. Castelijns[1], A.C. Moll[1], J.C. Dorsman[1], P. de Graaf[1]; [1]Amsterdam/NL, [2]Essen/DE, [3]Paris/FR, [4]Lausanne/CH, [5]Sienna/IT

Short Summary: Radiogenomics analysis in retinoblastoma reveals specific radiophenotype-genotype relations reflecting relevant individual genes and gene expression profiles.

Purpose/Objectives: To identify associations between qualitative non-invasive imaging features on MR imaging and gene expression profiles in retinoblastoma by applying radiogenomics analysis. In addition, a purpose of the study was to assess the ability of radiophenotypes to predict a previously defined gene expression signature associated with tumor progression and drug sensitivity.

Methods & Materials: In this retrospective study, radiogenomics analysis was performed at MR imaging of 65 retinoblastoma patients treated in VU University Medical Center. Retinoblastoma MR imaging features were defined in an imaging atlas and validated independently. Whole genome microarray analysis was performed on samples of enucleated eyes. Pre-treatment MR images were reviewed for 21 qualitative features by two readers blinded for genetic data. Imaging characteristics were correlated with matched whole genome expression data, accounting for multi-hypothesis testing. Unsupervised hierarchical clustering on imaging features and tumor samples was performed to create heatmaps of significant radiophenotype-genotype relations.

Results: Analysis of integrated data of imaging features and gene expression revealed 1336 statistically significant differentially expressed genes for specific imaging features. Significant associations were used to create heatmaps reflecting distinct pathways in cancer. Individual gene-to-imaging relations included the association of number of lesions (MR) and MYCN (p=0.0353), which amplification can initiate retinoblastoma. Overlapping imaging features diffuse growth pattern (MR) and plaque shape (MR) displayed overexpression of SERTAD3 (p=0,0025 and p=0,0492 respectively), which is known to be overexpressed in cancer cell lines. Smaller eye size (MR) correlated with PAX2 expression (p=0,0429), a gene associated with retina development. A previously described gene expression signature of 'photoreceptorness' of retinoblastoma could be identified using radiophenotypes. The photoreceptorness scale is associated with tumor progression and differential sensitivity to specific chemotherapy.

Conclusion: Radiogenomic associations can be identified between individual imaging features and gene expression profiles. Radiophenotype-genotype relations reflect relevant individual genes and cancer pathways. Radiophenotypes being associated with a gene signature for tumor progression and differential drug sensitivity implies a possible role in the future for radiogenomics in retinoblastoma for tumor staging and treatment decision making.

SOPS 1.2.

Follow-up of operated cancer of the oral cavity: don't worry, it's just a PET uptake!

G. Squassina[1], R. Maroldi[1], D. Farina[1], M. Ravanelli[1], F. Bertagna[1], L. Di Mare[2]; [1]Brescia/IT, [2]Rome/IT

Short Summary: Fifty-nine patients with operated cancer of the oral cavity were followed by PET and MRI. PET uptakes in the oral cavity had very low positive predictive value; all suspicious recurrences at PET in asymptomatic patients were proven to be false positive by follow-up or biopsy.

Purpose/Objectives: To assess diagnostic accuracy of FDG-PET/CT in local follow-up of surgically treated oral cancer.

Methods and Materials: One hundred and thirty seven PET scans (December 2011-Februar 2016) in 59 patients with previously operated cancer of the oral cavity were retrospectively reviewed. The surveillance protocol included PET and MR, alternated every 6 months. FDG uptake was classified in reports as functional (type 1), suspicious (type 2) or suggestive of recurrence (type 3). The cases in which PET uptake leaded to other diagnostic procedures (MR or biopsy) were classified as "positive". Follow-up (12 months) or histology were used as standard of reference for final diagnosis.

Results: In 48/59 patients FDG uptake in the oral floor/tongue was reported: 25/48 type 1, 14/48 type 2 and 9/48 type 3. Seven out of 9 PET scans with type 3 uptakes had been performed out of the routine follow-up schedule to stage clinically suspicious or proven recurrences: in all these cases, all imaging techniques were concordant about final diagnosis. In 10/16 PET scans performed during routine follow-up and showing type 2 or 3 uptake, MR was acquired to confirm or rule out recurrence: in all these cases, MR (and subsequent follow-up) were negative. PET in local follow-up had sensitivity, specificity, PPV and NPV of 100%, 70.7%, 36.8% and 100%. In 13/59 patients, follow-up PET identified nodal metastases (6/13, 2 in routine PET), distant metastases (6/13, 3 in routine PET) and second primary tumors (1 in a routine PET).

Conclusion: FDG-PET/CT shows optimal sensitivity and NPV but low specificity and PPV in local follow-up of operated cancer of the oral cavity.

SOPS 1.3.

Intravoxel incoherent motion imaging in head and neck cancer: a systematic review

D. Noij[1], R. Martens[1], T. Marcus[1], R. de Bree[2], R. Leemans[1], J. Castelijns[1], M. de Jong[1], P. de Graaf[1]; [1]Amsterdam/NL, [2]Utrecht/NL

Short Summary: In this systematic review we provide an overview of the literature on the use of intravoxel incoherent motion (IVIM) imaging in head and neck cancer (HNC). Despite large heterogeneity between studies we were able to identify the diagnostic and prognostic potential of this technique.

Purpose/Objectives: IVIM imaging is increasingly applied in the assessment of HNC. The purpose of this study was to determine the diagnostic and prognostic performance of IVIM in HNC by performing a critical review of the literature.

Methods and Materials: Pubmed and EMBASE were searched until April 2016. The only included search terms were "(IVIM OR ((intra-voxel OR intravoxel) AND incoherent AND motion))" in order to be as sensitive as possible. Studies were classified as diagnostic and/or prognostic. Data on the study and patients characteristics, the imaging protocol and diagnostic or prognostic outcomes were extracted by two independent reviewers.

Results: Due to large heterogeneity it was not possible to perform a meta-analysis. For our qualitative analysis we included 10 diagnostic studies, 5 prognostic studies and 2 studies assessing both. The most commonly used sequence was spin-echo echo planar imaging and a median of 10.5 b-values were used. Inclusion of low b-values is important for non-linear fitting of the signal. All but three studies included at least 4 b-values below b=200 s/mm2. The Levenberg-Marquardt algorithm was most commonly used for image fitting. With combinations of IVIM-parameters SCC, lymphoma, malignant SG tumors, warthin tumors and pleiomorphic adenoma can be reliably separated from each other. Low pre-treatment D and an increase in D during treatment was associated with a favorable response to treatment. D* appears to the least stable parameter and the parameter with the lowest prognostic value.

Conclusion: The use of multiparametric IVIM imaging has most diagnostic potential in HNC. Both D and f appear to have most prognostic capacity, while D* is the least stable and has the lowest prognostic value. Studies are very heterogeneous in terms of imaging protocols, outcome measurements and reference standards. Future research should focus on finding the optimal IVIM protocol. When assessing diagnostic and prognostic properties of IVIM, authors should use uniformly accepted study methods and larger patient populations.

SOPS 1.4.

Do quantitative diffusion weighted MRI parameters reflect human papilloma virus status in oropharyngeal and oral cavity head and neck squamous cell carcinoma?

V. Lenoir, T. De Perrot, M. Domingos, S. Stefanelli, P. Dulguerov, M. Pusztaszieri, M. Becker; Geneva/CH

Short Summary: Our study shows that quantitative DWI parameters chow significant differencies between HPV+ and HPV- HNSCCs reflecting their distinct histopathological microstructure.

Purpose/Objectives: Infection with the human papilloma virus (HPV) is a well-established cause for the development of head and neck squamous cell carcinoma (HNSCC). The purpose of this retrospective study was to compare quantitative diffusion-weighted imaging (DWI) parameters in HPV positive (HPV+) and HPV negative (HPV-) HNSCC based on radiologic-pathologic correlation.

Methods and Materials: 89 lesions in 87 consecutive patients (mean age = 65 years) with primary oropharyngeal (n= 41) and oral cavity (n= 48) HNSCC underwent MRI with routine anatomic and DWI sequences. Apparent diffusion coefficient (ADC) maps were calculated. Measurements were obtained by contouring the largest tumor areas on two consecutive slices. A voxel by voxel histogramm analysis was performed for ADC values. Images and quantitative data were analyzed by two experienced readers who were blinded to the standard of reference, which included histology and HPV status in all tumors.

Results: There were 17 HPV+ and 72 HPV- HNSCCs. 53% of HPV+ tumors and 83% of HPV- tumors were keratinizing HNSCC, whereas 47% of HPV+ and 17% of HPV- cancers were of the non-keratinising subtype ($p<0.02$). The mean tumor diameter was 30mm in HPV+ and 20mm in HPV- HNSCC ($p<0.05$). Mean and median ADCs were significantly lower in HPV+ (1010x10-6mm2/s and 964x10-6mm2/s) than in HPV- tumors (1143x10-6mm2/s and 1116x10-6mm2/s, $p <0.05$), whereas kurtosis and skewness were significantly higher in HPV+ (1.598 and 0.975) than in HPV- (0.677 and 0.535) cancers, respectively ($p<0.001$).

Conclusion: Significant differences in quantitative DWI parameters of HPV+ and HPV- HNSCCs exist reflecting their distinct histopathological microstructure.

SOPS 1.5.

The role of diffusion-weighted imaging at high b values in differentiation between benign and malignant cervical lymph nodes

T. Eldes, E. Zengin, F. Beyazal Celiker, O. Celebi Erdivanlı, M. Beyazal, M. Celiker, E. Dursun; Merkez - Rize/TR

Short Summary: Diffusion weighted imaging at high b values could be a good non-invasive method for differantiating malignancy from benign lesions in cervical region.

Purpose/Objectives: In association with detailed history and physical examination, novel imaging modalities are promising for the differential diagnosis of lymph adenopathy (LAP) as a non-invasive approach. We aimed to explore the role of diffusion-weighted imaging (DWI) for differentiation of malignant from benign lymph nodes in the cervical region.

Methods and Materials: Thirty-nine subjects with 73 enlarged lymph nodes in the neck were included. Subjects were assessed with the axial T1-weighted turbo spin echo (TSE), T2-weighted turbo inversion recovery magnitude, post-contrast T1-weighted TSE and DWI echo planar images with 1.5 T 32 channels Magnetom Aera (Siemens Healtcare Global). Quantitative ADC values were obtained from each value with the help of ROI. ADC values (b:0-1000 s/mm^2, 0-2000 s/mm^2 and 0-3000 s/mm^2) were compared with histopathologic results.

Results: After detailed investigation, 20% of 73 lymp nodes (8 hodgkin lymphoma and 7 metastatic lymph nodes) was reported as malignant. Among benign, 88% was reactive and, the remainders was granulomatous lymph nodes. The cut-off value was determined as 0.886x10^{-3} mm2/s (b: 0-1000), 0.705x10^{-3} mm2/s (b:0-2000) and 0.623x10^{-3} mm^2/s (b:0-3000) for differentiating malignancy from benign lesions. With these results, the sensitivity was 93% and the specifity was between 55% and 60% for all ADC values. The median ADC values according to the final diagnosis are summarized in table 1. There was a significant difference between the b:0-1000, b:0-2000 and b:0-3000 ADC values among the groups (p=0.032, p=0.005, p=0.008, respectively). The most signficinat difference was obtained between Hodkin lymphoma and reactive lymph nodes for ADC values (p=0.033, p=0.007, p=0.006).

Table 1. The median ADC values according to final diagnosis of LAP

	b1000 s/mm^2	b2000 s/mm^2	b3000 s/mm^2
Reactive, n=51	0.976x10^{-3}	0.793x10^{-3}	0.663x10^{-3}
Granulomatous, n=7	0.863x10^{-3}	0.652x10^{-3}	0.634x10^{-3}
Hodgkin, n=8	0.649x10^{-3}	0.477x10^{-3}	0.398x10^{-3}
Metastatic, n=7	0.844x10^{-3}	0.703x10^{-3}	0.579x10^{-3}

Conclusion: ADC values at different DWI might be a good predictor for differentiating malignant from benign lesions in neck region. Before daily clinical use, larger studies are needed in order to explore certain cut-off values for this differentiation.

SOPS 1.6.

Diagnostic accuracy of MRI techniques for treatment response evaluation in patients with head and neck tumours, a systematic review and meta-analysis

A. van der Hoorn, P.J. van Laar, G.A. Holtman, H.E. Westerlaan; Groningen/NL

Short Summary: The diagnostic accuracy of MRI is improved using ADC data in treated head and neck tumour patients.

Purpose/Objectives: Novel advanced MRI techniques are investigated in treated patients with head and neck tumours as conventional anatomical MRI is unreliable to differentiate tumour from treatment effects. As the diagnostic accuracy of both MRI techniques during or after treatment is unknown, we performed a systematic meta-analysis.

Methods and Materials: We searched studies reporting diagnostic accuracy of an anatomical, diffusion, perfusion or spectroscopy MRI to identify tumour progression confirmed by histology or imaging follow-up in treated head and neck tumour patients in PubMed, EMBASE and Web of Science from their first record till September 23th 2014.

Study inclusion and data selection were done by two authors independently. True positives, false positives, false negatives, true negatives were extracted. Studies were excluded if a 2x2 table could not be constructed. The Quality of Diagnostic Accuracy Studies checklist (QUADAS-2) was used to assess study quality. Meta-analysis was performed using bivariate random effect models when ≥ 5 studies per test were included.

Results: We identified 16 relevant studies with anatomical MRI and ADC. Because all included studies showed high risk of bias in ≥1 QUADAS-2 domain, the quality of the studies was moderate. Pooled analysis of anatomical MRI of the primary site (11 studies, N=854) displayed a sensitivity of 84% (95%CI 72-92%), specificity of 82% (95%CI 73-89%), positive likelihood ratio of 4.6 (95%CI 2.7-7.9) and negative likelihood ratio of 0.19 (95%CI 0.10-0.37). ADC of the primary site (5 studies, N=287) showed a pooled sensitivity of 89% (95%CI 74-96%), specificity of 86% (95%CI 69-94%), positive likelihood ratio of 6.1 (95%CI 2.5-15.1) and negative likelihood ratio of 0.13 (95%CI 0.05-0.34). Data for the nodal site were in the same range as the data for the primary site for both the anatomical MRI and the ADC data (Figure 1C-D), but were too few to calculate pooled estimates.

FIGURE 1 – Forest plots with diagnostic accuracy of anatomical MRI and ADC for primary tumour and nodal sites

A. Anatomical MRI primary site

Study	TP	FP	FN	TN	Sensitivity (95% CI)		Specificity (95% CI)	
Bhatia et al., 2010.[17]	11	4	8	38	58	(33-88)	90	(77-97)
Chan et al., 2006 group A.[18A]	21	3	1	9	95	(77-100)	75	(43-95)
Chan et al., 2006 group B.[18B]	3	11	1	197	75	(19-99)	95	(91-97)
Chong and Fan, 1997.[19]	5	7	4	29	56	(21-86)	81	(64-92)
Comoretto et al., 2008.[20]	27	4	1	31	96	(82-100)	89	(73-97)
King et al., 2013.[24]	9	7	0	21	100	(66-100)	75	(55-89)
Ljumanovic et al., 2008.[26]	25	13	1	41	96	(80-100)	76	(62-87)
Ng et al., 2010.[27]	25	7	4	143	86	(68-96)	95	(91-98)
Tshering Vogel et al., 2013.[28]	13	12	5	16	72	(47-90)	57	(37-76)
Vandecaveye et al., 2010.[29]	6	6	2	16	75	(35-97)	73	(50-89)
Yen et al., 2003.[31]	13	26	8	20	62	(38-82)	43	(29-59)

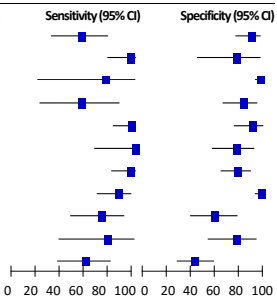

B. ADC primary site

Study	TP	FP	FN	TN	Sensitivity (95% CI)		Specificity (95% CI)	
Gouhar and El-Harir, 2011.[21]	11	1	2	7	85	(55-98)	88	(77-100)
Hong et al., 2013.[22]	16	40	7	71	70	(47-87)	64	(54-73)
Hwang et al., 2013.[23]	19	4	1	9	95	(75-100)	69	(39-91)
King et al., 2013.[25]	10	4	3	13	77	(46-95)	76	(50-93)
Tshering Vogel et al., 2013.[28]	17	0	1	21	94	(73-100)	100	(84-100)
Vandecaveye et al., 2010.[29]	8	1	0	21	100	(63-100)	95	(77-100)

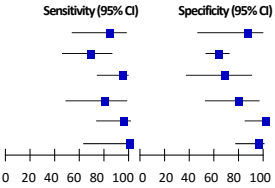

C. Anatomical MRI nodal site

Study	TP	FP	FN	TN	Sensitivity (95% CI)		Specificity (95% CI)	
Berrak et al., 2011.[16]	13	2	2	1	87	(60-98)	33	(1-91)
Comoretto et al., 2008.[20]	19	4	2	38	90	(70-99)	90	(77-97)
Ng et al., 2010.[27]	22	5	3	149	88	(69-97)	97	(93-99)
Vandecaveye et al., 2010.[29]	6	11	3	30	67	(30-93)	73	(57-86)

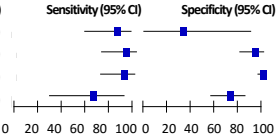

D. ADC nodal site

Study	TP	FP	FN	TN	Sensitivity (95% CI)		Specificity (95% CI)	
Berrak et al., 2011.[16]	11	0	4	3	73	(45-92)	100	(29-100)
Vandecaveye et al., 2010.[29]	7	5	2	36	78	(40-97)	88	(74-96)

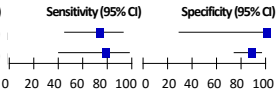

Diagnostic accuracy and the 2x2 table is displayed with true positives (TP), false positives (FP), false negatives (FN) and true negative (TN). Sensitivity and specificity with the 95% Confidence intervals (CI) are given.

Conclusion: The higher diagnostic accuracy of ADC values over anatomical conventional MRI emphasize the importance to perform a diffusion sequence with ADC maps in the standard imaging follow-up of treated patients with head and neck tumours.

SOPS 1.7.

MR imaging after nasopharynx endoscopic resection (NER): normal findings and complications.

I. Zorza, D. Farina, M. Ravanelli, R. Maroldi, V. Rampinelli, A. Schreiber; Brescia/IT

Short Summary: Imaging findings after 26 NERs are described. Normal MR findings are predictable, mainly depending on kind of surgery, and greatly differ from imaging findings in complications (osteomyelitis and abscesses).

Purpose/Objectives: To evaluate MRI findings after nasopharynx endoscopic resection (NER) -used as salvage therapy in recurrent nasopharyngeal carcinoma or as primary treatment of radio-resistant histotypes- focusing on normal findings and complications

Methods and Materials: A review of MR post-treatment imaging (performed within 1 years from surgery) was made in 26 consecutive patients submitted to NER between 2006 and 2015 in Brescia. NER are classified in 3 types, according to the extent of the resection: type 1, limited to postero-superior nasopharyngeal wall without bone resection; type 2, resection extended superiorly to the floor of sphenoid sinus; type 3, resection extended to the lateral nasopharyngeal wall, including the cartilaginous portion of the Eustachian tube. In some cases reconstruction flap was necessary to cover the surgical defect.

Results: NER type 3 was performed in 21/26 patients, NER type 2 in 4/26 and NER type 1 in 1/26. Reconstruction flaps were used in 18/26 patients: temporo-parietal fascial flaps (TPFF) in 11/18and Hadad flap in 7/18. Nasopharyngeal walls appear straightened after NER, regardless the type of resection/reconstruction performed. Discrimination between TPFF and Hadad flap is based on thickness and on T2 signal intensity, both lower in the latter. In patients with long-term follow-up, thinning of the flap can be observed, due to decreased edema. Mild bone changes of the residual sphenoid body and clivus (sclerosis, enhancement) and soft tissue edema in masticator space are commonly seen in uncomplicated patients. Six post-operative complications (4 osteomyelites of the cranio-cervical junction, 2 abscesses) were detected at MRI in 5 patients: osteomyelitis appears as diffuse abnormality and vivid enhancement of bone marrow signal (reflecting edema); cortical defects are sometimes seen. Abscesses are displayed as collections of heterogeneous unenhancingnecrotic debris surrounded by inflammatory rim-enhancement.

Conclusion: Normal post-NER imaging findings are predictable and depend on NER type, reconstruction technique and eventual complementary or previous radiotherapy. Typical post-NER complications are osteomyelitis of the cranio-cervical junction and retropharyngeal abscesses and can be effectively detected and monitored by MRI.

SOPS 1.8.

Adenoid cystic carcinoma of the head and neck region – morphologic characteristics in MRI

S. Greschus, F. Albert; Bonn/DE

Short Summary: Adenoid cystic carcinoma is a rare entity and knowledge about tumor morphology is essential for recognition of tumor recurrence and metastatic disease which can occur more than 15 years after primary diagnosis. The study analyses the morphologic behavior of this tumor entity in MRI which differs significantly from the more frequent squamous cell carcinoma.

Purpose/Objectives: Adenoid cystic carcinoma (ACC) is a rare tumor entity of the head and neck region and therefore the number of publications concerning radiological data is small. Objective of our study was the morphological characterization of the tumors in magnetic resonance imaging (MRI) in our patient collective.

Methods and Materials: Full-text search in the radiological data base for over the last ten years was performed. Patients who were diagnosed with primary or recurrent ACC and underwent MRI were identified. Morphologic criteria like T1 signal, T2 signal, contrast enhancement and homogeneity were analyzed qualitatively and semiquantitatively (signal intensity [SI] of the tumor compared to the pterygoid muscle). ADC was measured.

Results: 50 patients with the histopathological diagnosis of ACC could be identified. Most frequent primary location was the parotid gland (9/50) followed by the submandibular gland (7/50) and soft palate (7/50). 15 patients underwent MRI and could be included into the morphological analysis. All tumors showed a moderate to high T2 signal compared to the muscle (rel. SI 3.9 ± 2.1). T1 signal was isointense or slightly hyperintens to muscle (rel. SI 1.4 ± 0.7). The tumors showed marked enhancement (rel. SI 2.0 ± 0.3). Mean ADC was 1.6 ± 0.4 SD. 14/15 tumors exhibited necrosis or cysts. Noticeably 10/15 tumors presented with a hypointense rim in T2 surrounding the tumor and 12/15 had intrinsic hypointense septations.

Conclusion: Adenoid cystic carcinoma presents with a characteristic morphology differing markedly from the much more frequent squamous cell carcinoma. The tumor matrix is hyperintense in T2, shows marked enhancement, cystic or necrotic regions and frequently a T2 hypointense pseudocapsule. Remarkably the ADC seems to be much higher than in other malignant tumors and should not be misinterpreted as non-malignant. Knowledge of the morphology is important especially for the early recognition of tumor recurrence and metastatic disease.

SOPS 1.9.

SPECT-CT for identification of sentinel lymph nodes in early stage oral cancer

I.J. den Toom[1], A. van Schie[2], S. van Weert[2], O.S. Hoekstra[2], K.H. Karagozoglu[2], E. Bloemena[2], R. de Bree[1]; [1]Utrecht/NL, [2]Amsterdam/NL

Short Summary: SPECT-CT as imaging modality in sentinel lymph node biopsy in patients with early stage oral cancer

- has the potential to detect more SLNs than planar lymphoscintigraphy alone which results in upstaging of the neck in 3% of the patients
- provides better topographical orientation for the surgeon
- poorer accuracy in floor of mouth tumors has not been resolved by SPECT-CT

Purpose/Objectives: To estimate the role of Single Photon Emission Computed Tomography with Computed Tomography (SPECT-CT) in the identification of sentinel lymph nodes (SLNs) in patients with early stage (T1-T2) oral cancer and a clinically negative neck (cN0).

Methods and Materials: In addition to planar lymphoscintigraphy SPECT-CT was performed in 66 consecutive patients. Planar images only and combined with SPECT-CT images were retrospectively compared for detection of SLNs and anatomically localisation of SLNs by an independent nuclear physician, surgeon and investigator.

Results: Identification rate for both imaging modalities combined was 97% (64/66). SPECT-CT identified 15 additional SLNs in 14 patients (22%), particularly patients with a floor of mouth tumor. In 2/15 (13%) of these SLNs a metastasis was found and importantly these metastases were the only positive SLNs in these patients.

SPECT-CT was considered to add evident anatomical information in 2 patients (4%). Four hot spots in 3 patients initially scored as SLNs on planar lymphoscintigrams were scored as non-SLNs when SPECT-CT was added. There were 4 false negatives in this cohort.

Conclusion: The addition of SPECT-CT to planar lymphoscintigraphy is recommended for the identification of more SLNs and better topographical orientation for surgery in sentinel lymph node biopsy for early stage oral cancer.

NHS 1.1.
Elastography: Thyroid and more
K.S.S. Bhatia, Hong Kong/HK

Short Summary: US elastography describes US-based techniques that measure tissue elasticity or stiffness non-invasively. Since its introduction on US machines a decade ago, USE has been under intense investigation for tissue characterisation.

In the head and neck, USE research has focused on characterization of thyroid nodules, where over 100 pilot studies and several meta-analysis indicate that malignant thyroid nodules, in particular papillary carcinomas, are firmer than benign nodules (Figs.1&2).

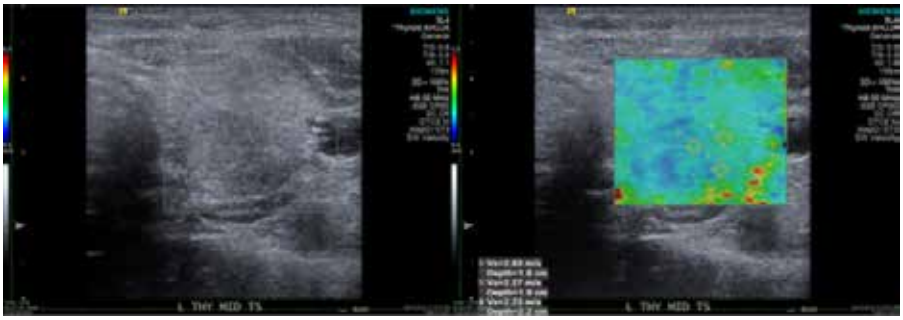

Fig 1. Benign thyroid nodule displaying low stiffness values on USE.

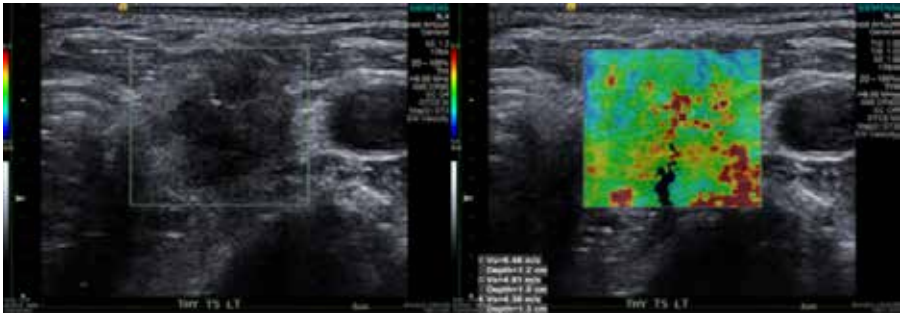

Fig 2. Papillary thyroid carcinoma displaying high stiffness values on USE.

However, the role of thyroid USE is controversial, which partly reflects widely discrepant accuracy data between published reports. Nevertheless, investigators with optimistic results have proposed that thyroid USE is a useful adjunct to conventional US by raising the negative predictive value for malignancy, which may reduce the rate of needle aspiration biopsies performed in otherwise sonographically indeterminate nodules.

USE has also been explored for characterization of cervical lymph nodes, salivary masses, parathyroid adenomas, diffuse pathologies of salivary glands and the thyroid, and post radiation complications in the neck.

This talk outlines the basic principles of USE and technical aspects including pre-compression, quality assurance, pitfalls and artifacts. The current evidence and future directions for head and neck USE will be summarized. The main focus will be on thyroid USE although evidence in other head and neck tissues will also be discussed.

Take Home Points:

US elastography (USE) measures and displays tissue stiffness or elasticity properties.

USE can be divided into strain and shear wave elastography techniques.

Thyroid USE may be a useful adjunct to conventional US for predicting benignity in thyroid nodules and thus lowering the rate of diagnostic needle aspirations performed in otherwise sonographically indeterminate nodules.

USE is under investigation for other indications including characterising salivary masses, cervical lymph nodes, diffuse salivary and thyroid diseases and post-RT changes.

US elastography is an operator dependent technique.

Various pitfalls and artifacts in USE need to be understood in order to optimize the accuracy of the technique.

USE technologies are proprietary and differ considerably between machine manufacturers, which influences the generalisability of published USE accuracy results.

SS 2.1.
Thyroid cancer, facts and figures: An overview

R. Evans, Cardiff/UK

Short Summary: Whilst thyroid nodules are ubiquitous on imaging; thyroid cancer remains a rare diagnosis, in the context of the frequency of nodular change within the thyroid. However within the Western world, the incidence of thyroid carcinoma is increasing, an incidence of 1.5 cases per 100,000 population was quoted in 1973, however in 2009 the incidence has risen to 7.5 cases per 100,000. (Ref 1)

The increased incidence of thyroid carcinoma (primarily papillary carcinoma of the thyroid) can be correlated to the increased use of imaging and in particular high-resolution imaging in the form of ultrasound and associated FNA/ultrasound guided FNA within the Western world.

However whilst the incidence has increased, mortality remains unchanged.(Ref 2) Papillary carcinoma makes up 85% of thyroid cancers, the increased reported incidence is primarily in small (less than 2 cm in diameter) papillary carcinomas, which are typically indolent tumours with a quoted twenty-year mortality of 1-2%.

The principle of Overdiagnosis in the context of thyroid cancer and thyroid imaging is thus highly relevant. To quote from Dr H Gilbert Welch, in his excellent editorial "Responding to the Challenge of Overdiagnosis"(Ref 3) the problem that exists for radiologists is to "sort the wheat from the chaff, minimising the cascades of diagnostic testing and the side effects of excessive intervention".Whilst the number of hemi-thyroidectomies in the United States of America has increased by 60% over the past decade(Ref 3), the underlying fact that mortality for thyroid carcinoma has not changed, morbidity is unlikely to remain stable and logically will have significantly increased.

Guidelines for thyroid imaging eg BTA guidelines UK,2014,Ref 4) attempt to standardise a diagnostic approach to imaging the thyroid and raising diagnostic thresholds. As always in radiology, the radiologist needs to question their own practice, and use imaging to provide the best care for their patients.

Take Home Points: This presentation and the other presentations/discussions in this session will aim to address the issues:

1. How can we best serve the patient with a thyroid mass?
2. An understanding of the relevant signs of nodular thyroid disease and thyroid cancer and the implications for the patient.

SS 3.1.
Clinical aspects of hyperparathyroid disease

J. Kievit, Leiden/NL

Short Summary: The spectrum of hyperparathyroid disease has changed after the last decennia, shifting from symptomatic disease to more and more asymptomatic, detected by screening. Many patients with 'asymptomatic' hyperparathyroidism are demonstrated from reduced quality of life at closer inspection, demonstrated both by disease specific, and by general quality of life questionnaire scores, which scores normalize after successful surgery. In addition, patients with (asymptomatic) hyperparathyroidism seem to be at excess risk of cardiovascular and other cause mortality, resulting in reduced overall life expectancy.

Appropriate biochemical workup is the basis of reliable diagnosis. Although imaging is neither necessary for diagnosis nor for justification of treatment, it may facilitate the surgical approach.

Take Home Points: Both morbidity and mortality data, as well as the results of (surgical) treatment, support the trend in recent guidelines to reduce the threshold for hyperparathyroidism treatment.

SS 3.2.
Diagnostic value of US, CT & MRI
P.S. Richards, London/UK

Short Summary: In experienced hands, US used alone or in combination with contrast agents, can be an accurate technique for detecting parathyroid gland enlargement. Used in conjunction with scintigraphy, it remains the mainstay investigation for primary hyperparathyroidism in many institutions across Europe.

However as targeted minimally invasive parathyroidectomy increasingly becomes the standard surgical treatment for primary hyperparathyroidism the need for precise and accurate preoperative localisation is paramount, as much to identify the 5 - 8 % of patients with multigland disease as to find a surgical target. In North America, where US is less utilised in general, there is a strong drive from towards 4D-CT to complement and increasingly to replace these techniques. However variability in the number of phases used for 4D-CT has emerged as there are significant concerns over radiation exposure.

In the past, MRI was unable to achieve adequate spatial and temporal resolution over the large FOV required for parathyroid imaging. However, a few recent studies have utilised fast imaging techniques such as time-resolved imaging with stochastic trajectories (TWIST) and new fat saturation techniques to overcome these technical limitations. Initial results are promising, with reported diagnostic accuracies and sensitivities equal to or greater than those reported for 4D-CT.

Take Home Points: Primary hyperparathyroidism is a benign condition in 99%.

The aim of surgery is cure at the first operation with minimum morbidity on the right patient with minimum cost and radiation exposure.

Minimally invasive surgery requires accurate pre-operative localisation not only to find a surgical target but to reliably exclude multigland disease which occurs in ~ 8 % in order to reduce the risk of redo surgery.

The thyroid specific dose of 4D-CT is 50 x MIBI. The lifetime risk of thyroid cancer in a 20 year old woman undergoing 4D-CT is 104 thyroid cancers / 100,000 exposed. This drops to 4/100,000 in 50 year old women. So reduce phases, age restrict and reserve for difficult cases.

4D-MRI is being developed and looks promising.

SS 3.3.
Contribution of metabolic imaging
B. de Keizer, Utrecht/NL

Short Summary: Metabolic imaging is done using planar scintigraphy, single photon emission computed tomography (SPECT) for gamma emitting radionuclides and positron emission tomography (PET) using positron emitting radionuclides.

Planar scintgraphy and SPECT-CT

For parathyroid scintigraphy and SPECT-CT the used radiofarmacon is Tc-99m-sestamibi. Tc-99m-sestamibi is absorbed by mitochondria of both thyroid and parathyroid cells. Hyperfunctioning parathyroids absorb the radiofarmacon faster than normal parathyroids and thyroid. Normal tyroid tissue and parathyroid tissue have different retention and washout. With more retention in parathyroid adenoma's. Using dual time point imaging 30 min and 2 hours post-injection parathyroid adenoma's can be detected with reported sensitivities varying between 54 and 100%. Sensitivity increases when SPECT-CT is added to, in our hospital approxiamtely 80%.

PET-CT

Recently it accidentaly was discovered that parathyroid adenoma accumulates F-18-fluorocholine (FCH), a PET tracer that is usually used for prostate cancer detection.Choline is an essential water-soluble nutrient necessary for processes like neurotransmitter syntheses (acetylcholine) and cell membrane synthesis. FCH accumulates intensely in parthyroid adenomas. Due to the intense accumulation and higher resolution of PET compared to SPECT (optimal resolution PET approximately 4 mm vs SPECT 10 mm) FCH PET has a higher sensiticity in detecting parathyroid adenoma, and has been used succesfully in patients with negative Tc-99m-sestamibi imaging or in cases wher SPECT and ultrasound are discordant.

Conclusion: SPECT-CT and PET-CT identifies parathyroid adenoma in the majority of patients. Succesfull identification of parathyroid adenoma allows minimal invasive surgery.

Take Home Points:

- differences between SPECT and PET tracers and imaging
- indications for FCH PET-CT
- goal is minimal invasive parathyroidectomy

SS 3.4.
Surgical treatment
J. Kievit, Leiden/NL

Short Summary: Recent insight in the elevated morbidity and mortality that is associated with hyperparathyroidism, have lower the threshold for treatment. Surgery has been demonstrated to not only be the most effective treatment, but also the most cost-effective one. In line with this, the threshold for surgery tends to go down in more recent guidelines. The preferred work-up for parathyroidectomy differs between institutions, with ultrasound and/or sestamibi scan being used widely.

Preoperative localization, in combination with a focused surgical approach and intraoperative PTH-assay more and more becoming the standard of care that combines the same effectiveness with shorter operating time and less morbidity.

Take Home Points: A well thought-out pre- and intraoperative strategy, in combination with ample endocrine surgical experience, are the corner stones of safe and effective treatment of primary and tertiary hyperparathyroidism.

SOPS 2.1.
Hypoglossal Canal Lesions: Differentiation of Craniocervical Junction Juxtaarticular Cysts and "Cystic" Hypoglossal Schwannomas
S. Weindling[1], C. Wood[2], J. Hoxworth[3]; [1]Jacksonville/US, [2]Rochester/US, [3]Phoenix/US

Short Summary: Comparison of CCJ JAC and Hypoglossal Schwannoma imaging features

Purpose/Objectives: We previously reported 12 patients in whom craniocervical junction juxtaarticular cysts (CCJJACs) caused ipsilateral hypoglossal palsy. In 5 of 12 CCJJAC patients, hypoglossal schwannoma (HS) was included within the radiology report differential diagnosis. We compare CCJJACs and HS imaging features to improve differentiation of these hypoglossal canal lesions.

Methods and Materials: We performed a 15 year enterprise wide radiology database retrospective review for reports containing the words "hypoglassal" AND "schwannoma", "tumor", "mass" or lesion". Imaging studies were reviewed for all cases in which the radiology report text was suspicious for HS, with HS confirmation and imaging characterization determined by consensus of the 3 participating Neuroradiologists.

Results: Eleven HS found in our retrospective review involved the premedullary cistern (10/11), hypoglossal canal (11/11) and extra-cranial carotid space (9/11), with 10/11 demonstrating secondary hypoglossal canal enlargement. On MRI T2-weighted images HS signal intensity (SI) was uniformly < CSF in 9/11, while 2/11 were heterogeneous containing components both < and = CSF SI. On enhanced T1-weighted images 5/11 HS demonstrated uniform enhancement. 6/11 HS contained "cystic" components, defined as intratumoral non-enhancing foci, which comprised < 25% (3), < 50% (2) or < 75% (1) of the lesion volume.

All 12 previously reported CCJJACs appeared as well-circumscribed extradural lesions causing 12th nerve encroachment limited to hypoglossal canal internal ostium (4/12) or extending into/through (8/2) the hypoglossal canal, with secondary hypoglossal canal erosion/remodeling on CT in 3/7. On MRI, all CCJJACs contained a dominant T2 hyperintense (= CSF) central cyst, comprising > 75% but < 100% of lesion volume, surrounded by thin, uniform rim enhancement.

Conclusion: Both CCJ JACs and HS may encroach the internal ostium or extend into the hypoglossal canal with secondary bony remodeling. When involving the pre-medullary cistern HS are intradural while JACs are extradural in location. HS are commonly partially cystic; however, non-enhancing foci comprised < 50% of lesion volume in 10 of 11, and all HS demonstrated some central or nodular peripheral enhancement. By comparison, all JACs contained a dominant central non-enhancing cyst (> 75% of lesion volume) surrounded by a uniform, thin enhancing rim.

SOPS 2.2.
Imaging findings in recurrent left cervical swelling syndrome

R. Hermans, S. Vanderschueren, B. Cassimon, V. Vander Poorten, O. Gheysens, W. Peetermans; Leuven/BE

Short Summary: Over a period of 18 years, 5 female patients presented in our hospital with recurrent left cervical swelling syndrome. Imaging showed pronounced left-sided neck edema, extending into surrounding regions. No obvious precipitating factors were identified. Biochemical analysis did not reveal abnormalities. Physical examination in between the acute phases was normal. The underlying condition might be an intermittent obstruction of the thoracic duct.

Purpose/Objectives: To report the imaging findings in recurrent left cervical swelling syndrome.

Methods and Materials: Over a period of 18 years, 5 female patients (age range 46-61 years) without significant medical history, presented in our hospital with an acute left cervical soft tissue swelling, spontaneously regressing over the next days. Four out of 5 patients experienced such episode at least twice. The clinical features and imaging findings were retrospectively analysed.

Results: All patients presented with acute swelling of the left supraclavicular neck region. Four patients had associated symptoms such as pain, difficulty swallowing and breathing, and/or hoarseness; none of the patients had fever.

A CT study, performed in the acute phase, showed left-sided neck edema, reaching up to level C3 or C4; in two patients, there was also retropharyngeal edema, extending up to level C2. The larynx, thyroid gland, proximal trachea and esophagus were slighlty deviated to the right in all patients. In two patients, the cervical part of the thoracic duct appeared wide. In all patients, the edema extended in the prepectoral and upper axillary region. Mediastinal edema was always present; the lowest extension was visualised in two patients, surrounding the carina. Pleural effusion was visible in three patients (bilateral in two, right-sided in one). All vascular structures appeared patent, there was no evidence for thrombosis.

No obvious precipitating factors were identified; in some instances, the swelling occurred soon after moderate physical activity, in one case after a fitness workout. Biochemical analysis did not reveal abnormalities. Physical examination in between the acute phases was normal.

Conclusion: Recurrent left cervical swelling syndrome is a rare entity, causing acute and self-limiting neck swelling. We hypothesize the underlying condition might be an intermittent obstruction of the thoracic duct, causing extravasation of chyle and subsequent interstitial edema.

SOPS 2.3.
Eosinophilic Angiocentric Fibrosis (EAF): CT and MRI findings from the largest reported single institution series

S. Jawad, S. Otero, S. Morley, T. Beale; London/UK

Short Summary: Eosinophilic Angiocentric Fibrosis (EAF) is a slowly progressive inflammatory disorder of the upper respiratory tract. To date, only 62 cases have been described in the English literature. We retrospectively review clinical and imaging finding in the largest single institution series of ten patients and find the nasal cavity and in particular the nasal septum are most commonly involved and the majority of patients have a characteritic MRI findings.

Purpose/Objectives: We present a case-based discussion of the pathology, presenting signs, imaging findings and management of EAF, and report the CT and MRI findings in the largest single institution series of ten patients.

Methods and Materials: We reviewed CT and MRI scans of ten cases between 2006 and 2016. Seven patients had CT and six had MRI. The following parameters were assessed: disease location, margin, CT attenuation and MRI signal characteristics.

Results: Eight patients had nasal cavity involvement and in all but one of these the nasal septum was involved. Nasal septal perforation was present in three cases. One patient had disease in both buccal spaces only and one patient had no detectable radiological abnormality. All margins were smooth. The CT findings were of non-specific soft tissue swelling at the site of involvement. Five of the six patients that underwent MRI had similar findings of poor enhancement, low T2 signal (with respect to skeletal muscle) and isointense T1 signal (with respect to grey matter). One case showed avidly and homogenously enhancing disease that returned high T2 and low T1 signal.

Conclusion: The CT appearances are non-specific and where possible MRI should be performed to characterise the extent of disease. EAF most commonly manifests as low T2 and isointense T1 signal. Nasal septal involvement is common in EAF and may progress to septal perforation. In the context of nasal perforation and low T2 signal elsewhere in the sinonasal tract, EAF is an important radiological consideration.

SOPS 2.4.

High specificity of Intravoxel Incoherent Motion (IVIM) parameter thresholds in differentiating benign and malignant salivary gland tumours

Y.L. Dai, K.H. Yeung, K.S.S. Bhatia, Hong Kong/HK

Objectives: To evaluate the intravoxel incoherent motion (IVIM) indices in different salivary gland tumours in order to differentiate between benign and malignant tumours.

Methods: We performed diffusion-weighted imaging (DWI) using 16 b-values (0-1500 s/mm2) in 58 patients with 59 salivary gland tumours (46 benign vs. 13 malignant) on 3T MRI and assessed perfusion (perfusion related incoherent microcirculation D*) and diffusion (pure diffusion coefficient D) related parameters in these tumours on the basis of IVIM theory.

Results: IVIM indices (D, D* and f values) were significantly different in benign salivary gland tumours including Warthin tumour and pleomorphic adenoma as compared with malignant salivary gland tumours. Warthin tumours had high D* values and low D values, while pleomorphic adenomas had low to intermediate D* values and high D values. Using the cutoff thresholds of high D* value (≥20 x 10-3 mm2/s) and high D value (≥1 x 10-3 mm2/s) allowed good identification of Warthin tumours and pleomorphic adenomas with high specificity (97.8% and 96.2% respectively). A combination of low D and D* values using the same thresholds allowed isolation of malignant salivary gland tumours with high negative predictive value (94.1%).

Conclusions: IVIM imaging may have an adjunct role to conventional imaging in differentiating between benign and salivary gland tumours with high specificity.

RC 1.1.

Non-oncologic peripheral nerve palsy: etiology and imaging findings in benign disorders

A. Borges, Lisbon/PT

Short Summary: Injury of cranial nerves may result in partial or complete loss of function which maybe motor, sensory or both. Affection of multiple cranial nerves and loss of specific functions of a single cranial nerve point out the anatomical site of injury. Demographic data and clinical findings help clinicians tailor the diagnostic tests needed to establish the cause of injury. Imaging plays a central role in this process as it can demonstrate both the consequence and cause of injury and, in certain cases, may help tailor treatment and predict patient's prognosis.

Benign causes of cranial nerve palsy include congenital, accidental and iatrogenic trauma, vascular disease (HT, diabetes, stroke, vascular malformations and neurovascular conflicts), infection, inflammation and tumors. Microvascular disease affecting CNs is often occult to imaging; trauma related CNs palsy is best appreciated with the use of CT, whereas infection, inflammation and nerve sheath tumors are best depicted on MRI. Use of appropriate technique and of high resolution imaging is mandatory to increase the diagnostic yield of imaging.

CNs denervation atrophy, is the hallmark of injury of motor nerves. In the acute setting it manifests by edema, best seen on fat-suppressed T2W images; in the subacute stage by contrast-enhancement and in the chronic stage by fatty replacement of muscle fibers and loss of volume.

Congenital lesions manifests by absence or hypoplasia of a particular CN; traumatic lesions by nerve impingement by a fracture, bony fragment or nerve hematoma, infectious/inflammatory lesions by diffuse, abnormal thickening and contrast enhancement of single or multiple CNs and tumors by an expansive contrast enhancing lesion. Vascular lesions range from nerve compression by an aneurysm or arteriovenous malformation, and nerve displacement or indentation by vascular loops at the root entry zone which are optimally depicted using angiographic techniques. Ischemic microvascular lesions are still a diagnosis of exclusion and should be sought in patients with vasculopathic risk factors.

Take Home Points:

- The use of appropriate technique is key to increase the diagnostic yield of imaging
- Multiple CNs involvement and loss of specific CN functions point out the site of injury
- Imaging can depict both the consequence and cause of CN injury

RC 1.2.
Perineural tumor spread: common pathways

B. Schuknecht, Zurich/CH

Short Summary: Tumors of the head and neck may spread by direct extension, hematogenous or lymphatic dissemination. Neoplastic invasion of nerves is a distinct entity with significant impact of surgical resectability, reduced recurrent free and overall survival

The hypothesis of reciprocal signaling interactions between tumor cells and nerves by neurotrophins, proteinases and adhesion molecules has replaced the lymphatic neural or low restance pathways theories.

It is relevant to distinguish perineural invasion from perineural spread. Perineural invasion is a histologic finding at the primary site, present when tumor cells lie within any of the layers of the nerve sheath (epi -, peri-, or endoneurium) or when tumor cells surround more than 33% of the circumference of the nerve. Perineural spread (PNS) however describes gross, radiologically evident extension of malignancy along „named“ craniocervical nerves.

In head and neck cancers PNS may be anticipated with adenoid cystic carcinoma (rates as high as 50 %). Due to higher prevalence PNS more commony occurs with squamous cell carcinoma (SCC) of mucosal and cutaneous origin. PNS is also a feature of basal cell carcinoma (incidence 2-3%), desmoplastic melanoma, lymphoma, leukemia and sarcoma.

PNS most commonly affects the trigeminal and facial nerve. Extension may be in a retrograde or antegrade direction Preexisting pathways account for continuity between CN V and VII.

Even if PNS is evident on CT with signs such as foraminal contour erosion or enlargement, MR is the preferred modality, Noncontrast T1 TSE and Gd enhannced with Dixon fat suppression technique depict loss of perneural fat, nerve thickening and foraminal enlargement. Submillimetric (0.5 -0.8mm) gradient echo(VIBE) sequences may identify addittional perineural venous plexus effacement and skip lesions and by MPR delineate additional branch or contralateral nerve involvement.

In comparison to histology MRI has a sensitivity of 83.3% to identify extension but underestimates spread in 13.3%.

Following adjuvant therapy, MR findings tend to persist. Therefore metabolic information by PET/MR may yield a higher diagnostic confidence for reassessment of perineural spread than MR.

Take Home Points:

- retrograde nerve extension in continuity or by skip lesions
- CN V and VII or both most commonly affected
- meticulous MR technique required

RC 1.3.
Neural imaging after surgery/radio(chemo)therapy

D. Farina, Brescia/IT

Short Summary: Patients treated for head and neck cancer may suffer with neuropathy that may involve cranial nerves, sympathetic chain or brachial plexus. Several mechanisms related to treatment may produce nerve damage: for example, surgical nerve transection may be part of a procedure or a iatrogenic complication. Though cranial nerves are relatively radioresistant, radiation induced neuropathy may occur with variable but non negligible incidence. In addition, both surgery and radiotherapy may produce submucosal fibrosis in the supra- and infrahyoid neck spaces, which is believed to be a substrate for nerve function impairment.

Chemotherapy induced neuropathy more commonly involves peripheral nerves: the underlying mechanism, infact, consists of axonopathy impairing the distal part of longer axons first. Only rarely, cranial nerves are involved, peculiarly after vincristine administration. MRI findings in post treatment neuropathies mainly consist – in the early/acute phase - of abnormal nerve thickness and/or signal intensity (namely edema related hyperintensity on T2 sequences and contrast enhancement); in the late/chronic phase quite often only hyperenhancement persists. Motor nerve injury may be indirectly heralded by denervation atrophy of the related muscles. Overall, imaging findings are quite non-specific and may overlap with several inflammatory non treatment-related conditions or with perineural tumor spread. The differential diagnosis may be further complicated by the presence of nerve deficits prior to treatment. Thorough knowledge of the clinical history (pre and post-treatment) and of the area and modality of treatment is therefore essential for adequate interpretation of imaging findings.

Take Home Points:

To understand the pathologic mechanisms of posttreatment neural damage

To understand imaging findings in posttreatment neural damage

SS 4.1.
Anatomical terminology of paranasal sinus and nose

T. Beale, London/UK

Short Summary: Sinonasal anatomy can be confusing especially in the radiology / anatomy textbooks as anatomical variants are the norm and there are multiple classification / grading systems in the literature, but it need not be.

I will try and simplify the process and give a template for reviewing / reporting this region.

By using a case base demonstration I will highlight some important anatomical landmarks and variants that must be mentioned in the report and communicated to the clinician. It is important that both the radiologist and the referring clinician speak the same sinonasal language.

Take Home Points:

Highlight clinically relevant anatomical variants

Understand the anatomy of the mucociliary drainage pathways

Speak the same anatomical language as your referrer

Understand how your report may change the patient's management

SS 4.2.
Paranasal and skull base endoscopic surgery: Clinico-radiological session

R. Maroldi, P. Nicolai, Brescia/IT

Short Summary: Paranasal sinus cancers are rare disease, accounting for about 5% of all head and neck malignancies. The variety of histological types and the overlapping pathological features with other entities constitute difficulties in pathologic interpretation, often requiring a skilled interpretation or a second opinion. Treatment of locally advanced disease relies on surgery and radiation therapy for operable disease, with a possible role for systemic treatment in selected histologies within a multimodal approach; unresectable paranasal sinus cancers are generally treated with a combination of radiotherapy and chemotherapy. Surgical treatment has evolved due to the progressive application of transnasal endoscopic techniques for naso-ethmoidal malignancies and due to innovative reconstructive techniques after resection of cancers of the maxillary sinus. Because of the rarity and complexity of this disease, multicenter trials represent an urgent need to improve prognosis and to reduce treatment-related effects

Take Home Points:

- Tumours affecting the nose, paranasal sinuses and adjacent skull base are rare
- They pose significant problems of management due their late presentation and juxtaposition to important anatomical structures such eye and brain
- The preoperative radiological and the postoperative pathological assessment are of utmost importance
- The increasing application of endonasal endoscopic techniques to their excision offers potentially similar scales of resection but with reduced morbidity.
- The importance of a multidisciplinary approach, adherence to oncologic principles with intent to cure and need for long-term follow-up is emphasised.

SOPS 3.1.

How to differentiate schwannomas from meningiomas of the IAM on a 3T MRI? Analyze endolymphatic and perilymphatic signal on a high-resolution gradient-echo T2 sequence!

A. Venkatasamy, F. Veillon, N. Meyer, S. Riehm, A. Charpiot, C. Debry, F. Proust; Strasbourg/FR

Short Summary: Perirlymphatic signal drop on a high resolution T2 weighted gradient-echo 3D (FIESTA-C) sequence on a 3T MRI is a helful sign to differenciate schwannomas from meningiomas, as the type of tumor changes the surgical management.

Purpose/Objectives: The aim of our study is to analyze the signal changes in the saccule, the utricle and the perilymph in schwannomas of the VIIIth nerve and meningiomas of the internal auditory canal on a high-resolution gradient echo T2- weighted 3D (FIESTA-C) sequence on a 3T MRI.

Methods and Materials: 203 schwannomas of the VIIIth nerve or meningiomas of the IAM are included and are compared to 60 healthy volunteers. The study was approved by the Ethics comittee and all patients undergo a high-resolution T2wi 3D FIESTA-C sequence on a 3T MRI. The schwannomas are separated prior to analysis according to their degree of obstruction. Two observers performed a visual analysis of the signal intensity of the different compartments compared to the controlateral side. For quantitative analysis, the signal intensity of the endolymph (saccule+utricle), perilymph (cistern+cochlea) and cerebrospinal fluid (CSF) are measured using Region Of Interest.

Results: 60 healthy volunteers (group 1, G1), 33 non-obstructive schwannomas (G2), 28 CSF-border schwannomas (G3), 129 obstructive schwannomas (G4) and 13 meningiomas (G5) were analyzed.

The Bayesian analysis showed no significant difference between G1 and G2 with a saccule/CSF (RSCSF) ratio, utricle/CSF (RUCSF) ratio and cistern/CSF (RCiCSF) ratio of 1.00 and a cochlea/CSF (RCoCSF) ratio of 0.90.

Obstructive schwannomas presented a strong perilymphatic signal drop with RCiCSF=0.63 and RCoCSF= 0.55 which was significantly different compared to normal ears.

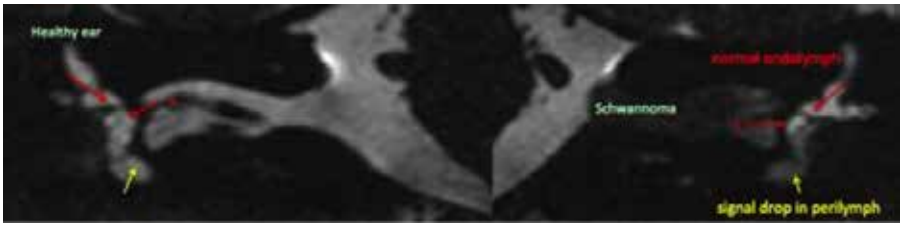

Figure 1: Obstructive schwannoma (G4)

Coronal FIESTA-C sequence of an obstructive schwannoma (G4) showing significant signal drop in the perilymph while the endolymph remains normal. In a normal healthy ear, both perilymphatic and endolymphatic fluid signals are normal

CSF-border schwannomas (RCiCSF=0.82, RCoCSF=0.73) and meningiomas (RCiCSF=0.81, RCoCSF=0.76) had a moderate perilymphatic signal drop and there was no significant difference between the two, but there was a significant difference versus groups G1, G2 and G4.

Figure 2: meningioma (G5)

Axial FIESTA-C sequence of a meningioma of the IAM showing a moderate drop in the perilymphatic signal (which appears grayish) compared to the controlateral side and compared to the strong signal drop of group 4 (illustrated in figure 1)

There were no changes of the endolymphatic signal.

Conclusion: This compartmental analysis of the liquids of the inner ear and especially the presence of a significant perilymphatic signal drop on a HRT2wi gradient-echo FIESTA-C sequence is a helpful tool in the differentiation of schwannomas from meningiomas on a 3T MRI, as the inner ear and the internal auditory canal are closely linked.

SOPS 3.2.

Sigmoid sinus diverticulum/dehiscence and dural venous sinus stenosis: Potential aetiologies for pulsatile tinnitus in patients with IIH?

A.L. Carlton Jones, J. Lansley, P. Riordan-Eva, W. Tucker, M. Eriksen, S. Connor; London/UK

Short Summary: We review the presence of sigmoid sinus diverticulum/dehiscence in idiopathic intracranial hypertension and its potential relationship to pulsatile tinnitus.

Purpose/Objectives: Pulsatile tinnitus (PT) is experienced by the majority of patients with idiopathic intracranial hypertension (IIH), however its origin remains uncertain. Turbulent venous flow secondary to transverse sinus stenoses (TSS) and/or sigmoid sinus wall abnormalities have been proposed as potential causes of PT.1,2 An association between between IIH and severe transverse sinus stenosis (TSS), has been well established.3 More recently imaging and clinical features of IIH have been described in PT patients with sigmoid sinus diverticulum/dehiscence (SSDD)4,5 suggesting that sinus wall abnormalities may also be implicated in the development PT in IIH. To test this theory we aimed to establish the relationship between SSDD and TSS in IIH patients with and without pulsatile tinnitus.

Methods and Materials: Consecutive patients with IIH (n=79; f=75, mean age 32) were identified from a clinical database. IIH was diagnosed by neurophthalmologists with support of CSF pressure measurements according to the modified Dandy criteria. Clinical data notes were reviewed for demographic and clinical data including a history of pulsatile tinnitus (n=42). CT vascular studies of the patients with IIH were compared with subjects (n=75 and age matched) without IIH or confounding pathology as controls. The presence of SSDD (diverticula and dehiscence separately) and transverse sinus stenoses were graded according to published criteria 3,4 following consensus review of the multiplanar reformats by two neuroradiologists.

Chi squared tests were used to compare the prevalence of severe (>75%) focal TSS and SSDD scores in IIH patients versus controls as well as in IIH patients with and without PT.

Results: Severe transverse sinus stenoses and sigmoid sinus dehiscences were more frequent ($p<0.05$) in patients with IIH versus controls however they were not more frequent in IIH patients with PT compared with those without PT.

Conclusion: Whilst our data corroborates previous studies demonstrating increased prevalence of SSDD and TSS in IIH, we did not establish an increased prevalence in those IIH patients with PT compared to those without PT. It therefore appears unlikely that these entities represent the structural correlate of PT in patients with IIH.

SOPS 3.3.

Superior semicircular canal dehiscence as a potential aetiology for pulsatile tinnitus in idiopathic intracranial hypertension

M. Eriksen[1], J. Lansley[2], P. Riordan-Eva[2], W. Tucker[2], S. Connor[2]; [1]Stavanger/NO, [2]London/UK

Short Summary: In our study we aimed to identify whether superior semicircular canal dehiscence (SSCD) could be a potential reason for pulsatile tinnitus (PT) in the patients with idiopathic intracranial hypertension (IIH).

Purpose/Objectives: Background/Purpose: Up to 65% of patients with idiopathic intracranial hypertension (IIH) experience pulsatile tinnitus (PT). The aetiology of the PT in these patients is uncertain, however it has been suggested that it may relate to venous sinus stenosis or pulsatile CSF. Subjects with higher body mass indices (a characteristic of IIH) are known to more frequently demonstrate superior semi-circular canal dehiscence (SSCD). Since SSCD may also present with PT, we speculated that SSCD could represent the structural correlate of PT in patients with IIH. In our study we aimed to determine whether SSCD was more prevalent in patients with IIH, and particularly in those IIH patients experiencing PT.

Methods and Materials: IIH was diagnosed by neurophthalmologists with support of CSF pressure measurements according to the modified Dandy criteria. Clinical notes were reviewed for a history of pulsatile tinnitus. CT studies of patients with IIH were compared with subjects without IIH or confounding pathology as controls. All CT studies were acquired with 0.625 mm collimation. The presence of SSCD was recorded following consensus review of the multiplanar reformats by two neuroradiologists.

Fisher's exact test was used to compare the prevalence of SSCD in IIH patients versus controls as well as IIH patients with and without PT.

Results: 79 patients with IIH were compared with 75 control subjects. 42 patients in the IIH group had a history of PT. We did not find a significant difference ($p>0.05$) in the prevalence of SSCD either between IIH patients with or without PT, or IIH patients versus controls.

Conclusion: We did not establish an increased prevalence of SSCD in IIH patients or in those IIH patients with PT. It therefore appears unlikely that this represents the structural correlate of PT in patients with IIH.

SOPS 3.4.
Malformation of the Leteral Semicircular Canal correlated with data from the audiogram

D. Le Foll, F. Veillon; Strasbourg/FR

Short Summary: Lateral semicircular canal (LSCC) malformation is one of the most common radiological inner ear malformations.

Purpose/Objectives: To demonstrate the existence of hearing loss proved by the audiogram correlated to the existence of a malformation of LSCC.

Methods and Materials: A retrospective study was conducted from November 2012 to December 2014. The malformated population includes patients presenting an isolated posterior labyrinthine malformation: 109 patients (53 men and 56 women, median age 44 years; Range 5-84). This population was confronted with a reference population, consulted for an unilateral temporal bone fracture with no previous abnormalities known of the audiogram, 27 patients and then 27 ears (16 men and 8 women, median age 44 years; Range 8-84). The primary efficacy criterion was to define whether there existed a pathology on the audiogram (SNHL, CHL or mixed deafness) correlated to a LSCC malformation.

Results: Among the 166 ears included, 39.1% had a sensorineural hearing loss (SNHL) (n=65), 39.1% had no hearing loss (n=65), 12.6% had a mixed hearing loss (n=21) and 9% had conductive hearing loss (CHL) (n=15). The results of an audiogram for each patient among the 57 included are: 17.4% of bilateral SNHL, 11.1% of normal hearing, 3.7% of bilateral mixed hearing loss and 0.9% of bilateral CHL. Among a bilateral malformed population of 57 patients, 89.9% of abnormality was found at the audiogram.

Conclusion: LSCC malformation is one of the most common radiological inner ear malformations associated with SNHL, mixed hearing loss and CHL in 89.9% of patient's cases.

SOPS 3.5.
Cochlear aperture development in relation to age

S.E. Sanverdi, M.A. Gurses; Ankara/TR

Short Summary: Development of inner ear is completed at the end of the second year of life. Cochlear aperture(CA) as a component of inner ear seems to be reached to its adulthood size in the early years of life, too. In this study size of CA has been analyzed in both children and adult population. The widest diameter of CA was measured on Computed Tomography(CT) scans and no statistically significance was found between in adults and children. It is suggested that findings might be helpful while evaluating temporal bone CT of patients with cochlear nerve agenesis and CA stenosis in daily routine.

Purpose/Objectives: To investigate the size changes of CA with increasing age.

Methods and Materials: Temporal bone CT images of 94 child and 117 adults(M/F: 114/97), a total of 422 temporal bones, were retrospectively analyzed. All CT studies of the temporal bone were performed on the same 16-channel multidetector CT scanner. The images were obtained with 0.5-mm collimation, 0.5-thickness, 100mA, and 120kV(peak). Axial-oblique reformatted images revealing the widest distance of the CA were obtained for the measurements. Images with extensive motion artifacts and patients with inner ear abnormalities (n=74 temporal bones) were not included in the study. Two radiologists, one is experienced in head and neck imaging, retrospectively and blindly measured the width of CA. For the comparison of the measurements in the different groups, and the relation with age and gender were analyzed with a dedicated statistical programme.

Results: Mean age was calculated 5.5 years in the children and 44.4 years in the adult group (with a range of 6 months-77 years). Mean width of CA was measured 1.71 mm in children and 1.81 mm in the adult group without a statistical significance (P=2). No side difference was found in the temporal bones of the same objects (P=1). Measurements revealed high interobserver agreement (r=0.86, P=0.2).

Conclusion: CA width did not differ between children and adult groups in our study. This statement might reflect that CA is an anatomical structure completes own development in the early term of life like many other inner ear structures. Further studies with larger populations and correlation of histological specimens are needed.

SOPS 3.6.

Perioperative scalar localization and cochlear trauma evaluation using high resolution CBCT and MRI image fusion

S. Peters[1], L. Oostveen[1], J. te Riet[1], L. Jacobs[1], W. Huinck[1], F. de Lange[1], E. Mylanus[1], B. Verbist[1, 2]; [1]Nijmegen/NL, [2]Leiden/NL

Short Summary: In order to localize individual cochlear implant electrode contacts and evaluate trauma, fusion of 3T MRI and perioperative CBCT was successfully achieved.

Purpose/Objectives: Computed tomography imaging of cochlear implant arrays faces many challenges: 1) postoperative imaging leaves little opportunity for correction; 2) imaging of separate electrode contacts is challenging since new array designs usually have smaller electrode contact spacing; 3) evaluation of cochlear trauma is difficult because cochlear structures (e.g. basilar membrane) are often hardly visible. Here, we present a proof of concept of a high resolution imaging strategy to localize individual electrode contacts and evaluate trauma by combining the relative strengths of MRI and perioperative CBCT.

Methods and Materials: A human cadaver head was implanted with a Cochlear Nucleus® Slim Modiolar Electrode (CI532) lead, containing 22 electrode contacts on 14mm active length. The head was scanned before implantation on a 3T MRI system (Siemens Magnetom Trio A Tim) and after implantation on a Siemens Artis Zeego system (3D DynaCT, voxel size 0.21 mm) in the operating room. To compare electrode visualization on CT, the head was also scanned on two regular CT systems: Toshiba Aquilion ONE VISION Edition and Siemens Somatom Sensation-64.

Fusion of MRI with DynaCT was performed with Siemens SyngoXWP VD10E software. Accuracy of automatic fusion was checked using predefined landmarks (horizontal/vertical semicircular canal, base of modiolus, nervus facialis genu anterior site). Mean Euclidian distances (mEd) of the landmarks on MRI and DynaCT were calculated: a resulting distance <0.5 mm was considered successful fusion. If necessary, images were manually adjusted to decrease mEd.

Results: DynaCT images clearly showed individual CI532 electrode contacts, as opposed to imaging on regular CT. Radiation dose was 0.8 mSv.

Fusion of cochlear structures on MRI and DynaCT images of the cadaver head yielded an mEd of 0.7 mm and 0.3 mm for automatic and manual fusion, respectively. Cochlear trauma was not observed.

Conclusion: Fusion of 3T MRI and DynaCT images can be successfully achieved to gain insight in electrode array position and possibly cochlear trauma perioperatively. The developed method is currently employed in a clinical study on patients receiving the CI532 lead. Radiation dose will be 0.1-0.8 mSv.

SOPS 3.7.
Preliminary Outcome of Cochlear Implantation in Children with Hypoplasia of the Cochlear Nerve

A. Giesemann, F. Götz, A. Illg, T. Lenarz, H. Lanfermann, D. Adams; Hannover/DE

Short Summary: Hypoplasia of the cochlear nerve is a rare MR-diagnosis in evaluation of cochlear implant candidates. It is often hard to differentiate from true aplasia of the cochlear nerve and in cases of very thin nerves the question remains, if the child will profit from a cochlear implant. Advances in resolution provide more detail in preoperative Imaging of nerve hypoplasia, the outcome however cannot be reliable predicted.

Purpose/Objectives: To evaluate the outcome of cochlear implantation in children with hypoplasia of the cochlear nerve and to analyze if best possible resolution is able to identify smallest nerve diameters that will still provide positive hearing results.

Methods and Materials: We identified 30 children with uni- or bilateral cochlear nerve hypo- or aplasia of whom 17 were implanted uni- or bilateral, giving 26 implanted ears with cochlear nerve hypo- or aplasia using pre-operative high resolution MR Imaging. Image resolution of the T2-weighted space-sequence was a 512er matrix in 3T in 7 patients (11 ears), a 384er matrix in 3T in 3 patients (4 ears) and a 512er matrix in 1.5 T in 7 patients (11 ears).

Results: All children presented with cochlear nerve hypoplasia or aplasia, in 15 ears the hypoplasia was severe or even a questionable aplasia – however depending on imaging resolution. Twelve ears of 26 achieved hearing results in CAP values between 1 and 8. The remaining ears do not show reaction on noise, three ears were explanted and eight ears are implanted too short for a definitive answer.

Conclusion: Predicting outcome of cochlear implantation in cochlear nerve hypoplasia remains difficult and results show unexpected good outcomes as well as a number of implantations without results. However the most difficult cases in imaging interpretation often seem to be difficult cases in judging the outcome as well.

SOPS 3.8.
Visibility of the discomallear ligament on high-resolution computed tomography of the temporal bone

E. Arkink[1], B. Verbist[1, 2]; [1]Leiden/NL, [2]Nijmegen/NL

Short Summary: The intratympanic part of the discomallear ligament (DML) may be visible on high-resolution computed tomography (CT) of the temporal bone.

Purpose/Objectives: The DML is a ligamentous structure sharing a common origin with the anterior mallear ligament (AML), with a rostrocaudal and lateral course through the petrotympanic fissure (PTF), that connects the malleus to the temporomandibular joint (TMJ) disc. Its existence has been disputed and its function is unclear. Its morphological features may relate to TMJ pain, auditory and TMJ dysfunction. The visibility of the intratympanic part of the DML on high-resolution CT has not yet been assessed.

Methods and Materials: We retrospectively examined CT studies of 104 temporal bones in 52 patients (aged 1-94 years of age) that underwent high-resolution temporal bone CT between July and September 2015 at a 320-MDCT volumetric scanner (Aquilion ONE, Toshiba). Temporal bones affected by conductive or mixed hearing loss were excluded (n=10). We assessed the presence of separate PTF canals for the DML and AML, measured the smallest DML canal diameter, and scored the intratympanic DML and AML prevalence using a 3-point scale (0=not visible; 1=possibly visible; 2=certainly visible).

Results: In n=94 temporal bones included in analyses, separate DML and AML canals through the PTF were identified in n=74 temporal bones (79%); a common canal for DML and AML was present in n=20 (21%). The median smallest DML canal diameter was 0.2 mm (range 0.0-0.8 mm). Intratympanic ligamentous structures were not discernible in n=21 due to middle ear cavity obliteration. In the remaining temporal bones (n=73), DML and AML were certainly visible in n=27 (37%) and n=63 (86%), respectively. They were possibly visible in n=21 (29%) and n=9 (12%), and not visible in n=25 (34%) and n=1 (1%), respectively. The DML was most often observed in those aged <50 years (55% certainly visible, 24% possibly visible).

Conclusion: This observational study shows that a separate DML canal through the petrotympanic fissure is visible in 79% and that the intratympanic part of the DML may be discernible from the AML on high-resolution CT scans. Knowledge of its normal appearance may help in identifying abnormalities that might explain TMJ pain, auditory and TMJ dysfunction.

SOPS 3.9.

Holes in the skull – The differential diagnosis of lytic skull lesions

M. Veiga, M. Diogo, J. Ramalho, C. Pinheiro, C. Perry da Câmara, C. Conceição; Lisbon/PT

Short Summary: Lytic skull lesions are often asymptomatic and incidentally discovered on radiological examinations obtained for unrelated reasons. A significant variety of etiologies are possible, including anatomical variants, congenital, inflammatory, neoplastic and traumatic. Clinical information and an accurate imaging evaluation with computed tomography (CT) and/or magnetic resonance imaging (MRI) are essential in the evaluation of these lesions. The purpose of this presentation is to briefly review the imaging characteristics of different skull lytic lesions, in order to guide the diagnosis and limit clinical differential diagnosis.

Learning Objectives: The main goal of this presentation is to perform an overview of the differential diagnoses of lytic skull lesions by evaluating the imaging characteristics that permit the correct identification and diagnosis.

Background: There are several conditions associated with lytic skull lesions. They are often incidental imaging findings, but sometimes may represent the reason to perform the exam. The combination of clinical information, as well as CT and MR imaging features, is essential for the accurate evaluation and differential diagnosis of these lesions. In adults, neoplasms represent the main etiology, especially metastasis or myeloma; in children, dermoid cysts and eosinophilic granuloma are the most frequent causes.

Imaging Findings or Procedure Details: Lytic skull lesions can be either solitary or multiple. The most common solitary lesions are due to normal anatomical variants, or secondary to surgical defects, trauma, dermoid or eosinophilic granuloma. It is however important to bear in mind the less common causes of skull “holes”, which include leptomeningeal cyst, metastatic disease, epidermoid cyst, multiple myeloma, histiocytosis or congenital malformations, such as encephaloceles. In the presence of multiple lytic lesions, main differential diagnosis includes metastasis, lymphoma, multiple myeloma, but other differentials like metabolic conditions should be considered. Examples of these entities are shown in this presentation.

Conclusion: Different imaging techniques allow the identification and characterization of lytic skull lesions. The recognition of particular imaging features is extremely important, as they often constitute valuable diagnostic clues to achieve the correct diagnosis.

NHS 2.1.

Ultra High Field MRI: challenges, safety and H&N applications

A. Webb, Leiden/NL

Short Summary: This talk will discuss the opportunities and challenges of 7 Tesla MRI for clinical radiological applications in general, and specifically for head and neck. Topics covered will include signal-to-noise and spatial resolution, image non-uniformities, and strategies for reduced power deposition. Clinically relevant applications will include ocular tumours, inner ear imaging, and protocols for imaging nerves.

Take Home Points:

High field MRI has progressed from a technology development stage to one in which clinical cases are routinely performed.

The major challenge with high field MRI is the non-uniformity of the transmitted magnetic field.

Applications in which spatial resolution is critical are most suitable for ultra high field MRI.

New high permittivity materials can be used to focus the MRI signal to regions of specific interest.

SS 5.1.

Otogenetics: Diagnosing hereditary hearing loss

S. Kant, M. Kriek, Leiden/NL

Short Summary: Until recently, genes were tested for abnormalities one by one. Exome sequencing now allows all genes to be simultaneously tested for abnormalities, thus considerably increasing the chance of finding the cause of a genetic disorder.

In practice, testing will initially focus on abnormalities in genes that are known to have a relationship with the condition being investigated. This is called 'targeted DNA testing'. If this does not result in a diagnosis, the remaining genes will be tested for abnormalities for as far as possible. This is known as 'exome-wide DNA testing'. As hereditary hearing loss is a polygenic disorder, the application of targeted and exome-wide DNA testing is highly appropriate for this patient group.

A specific diagnosis may have consequences for screening for additional medical problems, for treatment options and for reproduction choices.

Several cases will be presented in which either targeted DNA testing or exome-wide DNA testing has been performed, and the impact of the results on the patients and their relatives will be discussed.

Take Home Points:

- There are >100 genetic causes of hearing loss
- Testing for hereditary hearing loss is a balance between single gene analysis and targeted DNA testing / exome-wide DNA testing
- Establishing a genetic diagnosis may have (medical) consequences, other than hearing loss, for the patient and his/her relatives

SS 5.2.
Imaging findings in congenital hearing loss
J. Casselman, Bruges/BE

Short Summary: The cause of congenital hearing loss can be found at the level of the external auditory canal (EAC), middle ear (ME), inner ear (IE) or along the central auditory pathway (CAP). EAC and ME malformations are often associated and are best studied using high resolution MDCT or CBCT and the technique with the lowest radiation dose is preferred in very young children. Detection of subtle important malformations like the abnormal course of the facial nerve in EAC atresia or the exact status of the ossicles and windows in congenital conductive hearing loss can only be assessed in detail when thin reconstruction are made (MDCT - 0.1/0.2 mm) or when high resolution images are acquired (CBCT - 150 µm). Inner ear malformations most often occur isolated. Major IE malformations can be seen on CT but subtle cochlear incomplete partition and cochleovestibular nerve dysplasia/aplasia malformations can only be detected on MR. The CAP must also be verified in congenital SNHL to exclude malformations from the cochlear nuclei up to the auditory cortex, which can also cause congenital hearing loss. These are also better seen on MR making MR the imaging technique of choice to study the IE and CAP. CT is sufficient when congenital EAC malformations are depicted clinically or when otoscopy indicates ME problems. However, it is not always easy to clinically distinguish ME or IE causes in neonates and infants. Moreover the imaging studies are best performed under anesthesia/sedation. To avoid repetitive anesthesia/sedation it is therefore wise to perform both inital imaging studies during one session. Anyway both CT and MR are needed in most of the IE/CAP, cochlear implant/ brainstem implant patients and in “syndrome” patients in whom the EAC/ME/IE/CAP can be involved together. All the above will be discussed and illustrated.

Take Home Points:

Be familiar with the state of the art CT and MR techniques to study congenital hearing loss.

Learn which technique(s) should be used for which congenital ear malformations.

Known the most frequent causes of congenital hearing loss at the level of the EAC/ME/IE/CAP.

Learn which imaging findings are crucial to the surgeon in patients with congenital hearing loss.

SS 5.3.
Treatment options and postoperative imaging
B.M. Verbist, Leiden/NL

Short Summary: Developmental disorders of the temporal bone will lead to conductive, mixed or sensorineural hearing loss. Since hearing impairment has an impact on school or work performance, cognitive and emotional status and social connectivity, effective functional rehabilitation is considered a matter of critical importance. Hearing aids are beneficial for most people with mild to moderate hearing loss. However, in some patients they can't be worn because of anatomical malformations or chronic infection or they do not improve hearing sufficiently in case of poor air conduction or profound sensorineural hearing loss. Thanks to advances in auditory technology implantable devices have been developed for these patients. This is a rapidly evolving field and meanwhile the use of implantable devices has become well established in audiological rehabilitation.

In this lecture an overview of different implant types will be given: bone conduction hearing implant (BCHI), active middle ear implant (MEI), cochlear implant (CI) and auditory brainstem implant (ABI). Indications for implantation and working of these devices will be explained, postoperative imaging findings after successful surgery as well as complications will be illustrated and imaging-based outcome evaluation will be discussed. MRI compatibility will shortly be commented upon.

Take Home Points:

1. Implantable devices are well established treatment options in (congenital) hearing loss
2. Knowledge of ongoing developments in this area is of importance for accurate evaluation of postoperative images.

SOPS 4.1.
MR imaging of cranial nerves in the cavernous sinus: comparison between 3D-VIBE and contrast-enhanced 3D-CISS.
M. Ravanelli, D. Farina, R. Maroldi, E. Botturi, A. Marconi; Brescia/IT

Short Summary: Comparison of 3D-VIBEand CE-CISS in depicting cranial nerves within cavernous sinus was performed on 40 MR studies of the skull base. CE-CISS was superior to VIBE in imaging IV, V and VI cranial nerve.

Purpose/Objectives: MR imaging of the cavernous sinus is technically challenging because of its miniaturized anatomy. Three-dimensional sequences are the gold standard because capable of sub-millimetric spatial resolution in-plane and along slice-selection direction. This study is aimed to compare contrast-enhanced 3D VIBE (3D-VIBE), used in our standard protocol, and recently introduced contrast-enhanced 3D CISS (CE-CISS) sequences in depicting cranial nerves (CNs) within and adjacent to cavernous sinus.

Methods and Materials: 40 MR studies (1.5 T equipment) of the skull base were reviewed. Imaging protocol included 3D-VIBE and CE-CISS sequences, with isotropic spatial resolution ranging from 0.5 to 0.6mm. Visibility of intra-cavernous tract of III, IV, V1, V2 and VI CNs was qualitatively scored by an expert head and neck radiologist: 0=not visible, 1=low-quality depiction, 2=clearly depicted. Performance of two sequences was compared using Chi-squared and Friedman's test.

Results: Six of 80 cavernous sinuses were not assessable because involved by neoplastic disease. Third, IV, V1, V2 and VI CNs were visible (score 1 or 2) in 97%, 42%, 97%, 100% and 97% of cases with 3D-VIBE and in 100%, 85%, 100%, 100% and 100% of cases with CE-CISS (chi-squared $p<0.0001$ for IV CN, not-significant for other CNs). Mean scores for III, IV, V1, V2 and VI were respectively 1.86, 0.58, 1.35, 1.69, 1.65 for 3D-VIBE and1.99, 1.27, 1.66, 1.95, 1.95 or CE-CISS. CE-CISS was statistically superior to 3D-VIBE in depicting IV, V1, V2 and VI (Friedman's test $p<0.0001$, 0.01, 0.03, 0.02), while there was no statistical difference in visualizing III cranial nerve (Friedman's test $p=0.42$).

Conclusion: CE-CISS depicts IV-VI CNs within the cavernous sinus with higher quality than 3D-VIBE.

SOPS 4.2.

Diagnostic efficacy and therapeutic impact of computed tomography in the evaluation of clinically suspected otosclerosis

C. Dudau, F. Salim, D. Jiang, S. Connor; London/UK

Short Summary: CT demonstrates a high rate of alternative diagnoses in clinically suspected otosclerosis, 1:3

CT results in a high rate of targeted surgery in suspected otosclerosis, 1:4

CT limits exploratory surgery in patients with suspected otosclerosis

CT demonstrates clinically relevant extensions of otosclerosis

Endosteal extension of otosclerosis is predictive of lower bone conduction tresholds presurgically

The PPV of CT diagnosis of otosclerosis was 100%

Purpose/Objectives: To assess the diagnostic efficacy and therapeutic impact of CT in evaluating patients with clinically suspected otosclerosis.

Methods and Materials: CT scans performed over a 5-year period for clinically suspected otosclerosis were retrospectively reviewed. CT diagnoses were correlated with subsequent surgical management. For otosclerosis positive cases, clinically significant extensions of otosclerosis were correlated with audiometry and the CT diagnosis was correlated with surgical findings.

Results: Of 259 CT studies, 46% of patients were positive, 49% negative and 5% equivocal for otosclerosis. CT outcome influenced the decision to perform targeted surgery for otosclerosis, with 41% CT positive and only 4% CT negative patients undergoing stapedectomy. A relevant alternative CT diagnosis was evident in 33% of otosclerosis negative studies and one targeted surgery was performed for every 4 CT studies. When otosclerosis was demonstrated, clinically relevant extensions of otosclerosis were documented in 16% of ears. CT positive ears for otosclerosis could not be predicted form baseline clinical or audiometric criteria. Those with endosteal extension demonstrated lower bone conduction thresholds presurgically. The positive predictive value of CT diagnosis of otosclerosis was 100%.

Conclusion: CT demonstrated a high rate of clinically relevant diagnoses in both CT positive and negative for otosclerosis, and this frequently influenced surgical management. CT also added value by demonstrating clinically relevant extensions of the otosclerotic foci, some of which were predictive of audiometric parameters. A CT diagnosis of otosclerosis was strongly predictive of surgical findings.

SOPS 4.3.

Influence of voxel sizes and slice thickness for the assessment of semicircular canals: Comparison of Cone Beam CT and Multislice CT

K. Orhan[1], N. Nihal Yetimoglu Özdil[1], U. Seki[1], T. Ormeci[2]; [1]Ankara/TR, [2]Istanbul/TR

Short Summary: A recent development in radiology is the use of cone beam detectors in CT to obtain higher-resolution images. We sought to compare diagnostic value of a cone beam CT (CBCT) unit which is routinely used in clinical setup with current state-of-the-art multisection CT (MSCT) scanners.

Purpose/Objectives: The objective of this study was to evaluate and compare the influence of different voxel resolutions and various slice thickness of cone beam computed tomography (CBCT) and multislice computed tomography (MSCT) units for detection of semicircular anatomy and morphometry in-vitro.

Methods and Materials: 40 temporal bone of 20 skulls was scanned using a CBCT unit (Planmeca Promax 3D) and a 256 slice MSCT (Philips Brilliance iCT). CBCT images were obtained from in four isotropic voxel sizes (voxel size 0.100 mm3, 0.150 mm3, 0.200 mm3, 0,400 mm3) and in various slice thickness (0.10 mm, 0,15mm, 0,20mm, 0,40mm, 1mm, 2mm) while MSCT images were obtained both isotropic voxel (0.67 mm3) and anisotropic voxel settings in various slice thickness (0.625 mm, 1mm and 1.5 mm)

Various dimensions of semicircular canals (SSC) such as; width, height the internal width/height were measured. Moreover, angles between Superior SCC, Posterior SCC, Lateral SCC were also calculated. Moreover, the existence of pneumatization and dehiscences were evaluated in Superior SCC. In case of a possible dehiscence, a temporal bone bisection were performed in order to have definite dehiscence diagnosis. Kappa coefficients were calculated to assess both inter-observer agreements for each image set. T-test was used for pairwise correlations ($p<0.05$).

Results: The superior semicircular canal slightly wider than posteriors semicircular canals. The heights were similar without a significant difference (p>0.05). There was also no significant difference for the distance Superior SCC roof length according to sites (p>0.05). However, statistical significance was found for Superior and Lateral SCC height according to voxel sizes (p<0.05). No significant was found among angles of SCC (p>0.05). Significant difference was also found for detection of Superior SCC dehiscence according to voxel sizes (p<0.05).

Conclusion: 0.400 mm3 voxel-size was identified as the cut-off point for detection of some of semicircular canal anatomical structures. CBCT should be considered a reliable imaging modality for temporal-bone imaging.

SOPS 4.4.
MRI of acute mastoiditis: comparison of temporal bone imaging findings with CECT and with incidental pathology in MRI.

R. Saat, G. Mahmood, N. Brandstack, A. Laulajainen-Hongisto, J. Jero, A. Markkola; Helsinki/FI

Short Summary: Bright signal inside the mastoid air cells on T2-weighted images is a sensitive but unspecific feature of acute mastoiditis (AM), because it may also be present as an incidental finding that does not neccessarily indicate clinical mastoid infection.

Purpose/Objectives:

- To determine the incidence of different MR imaging findings in AM.
- To compare MRI features of clinical AM with those of incidental mastoid pathology in MRI.
- To asess diagnoctic performance of MRI in comparison to contrast-enhanced CT in AM.

Methods and Materials: MR scans of 35 adult and paediatric patients with clinical AM were retrospectively reviewed and compared to contrast-enhanced CT scans of AM patients (n=52, 27 of which were from the same patients), and to 34 MR scans (out of 2341 consecutive head or temporal bone scans) of age-matched controls with incidental T2-hyperintensity, covering > 50% of the mastoid cavity, and without any relevant clinical middle ear pathology.

Results: T2-hyperintensity, covering > 50% of the mastoid cavity, was detected in 94% of patients with AM. The same feature was incidentally present on head MR scans at a frequency of 4,6 %.

When compared to incidental findings, the intramastoid contents in clinical AM were hypointense to CSF on T2-WI in 86% vs. 6% (p<0.001), they showed diffusion restriction in 62% vs. 0% (p<0.001), and intense enhancement after intravenous administration of Gd contrast agent in 51% vs.0% (p<0.001).

Other, less frequent signs of clinical AM were perimastoid periosteal (69% vs. 3%, p<0.001) and perimastoid meningeal enhancement (43% vs. 3%, p<0.001), and signs of bone destruction on T2-weighted TSE images (49% vs. 0%, p<0.001).

Assessment of mastoid septal destruction in MRI showed moderate inter-observer agreement (κ=0,50) but this was not inferior to CT.

Intra- and extracranial complications were rare but reliable and clinically important signs of AM.

Conclusion: MRI provides several ways to assess intramastoid contents and soft-tissue changes in AM, and to differentiate incidental findings from clinical AM.

SOPS 4.5.
Magnetic resonance imaging of temporomandibular joint dysfunction - correlation with clinical symptoms, age, and gender

J. Avsenik, U. Lamot, P. Strojan, K. Šurlan Popovic; Ljubljana/SI

Short Summary: Temporomandibular joint (TMJ) dysfunction is a common condition, associated with pain, clicking, crepitus, restriction of motion, deviated jaw, headache, vertigo and tinnitus. Magnetic resonance imaging (MRI) is the primary imaging technique in the diagnosis, providing superior information of joint structures. Internal derangement, osteoarthritis, and effusion contribute to TMJ dysfunction. Early diagnosis is important because therapy is often inefficient in advanced phase. We aimed to determine which of the MRI morphological manifestations correlate with the signs and symptoms of TMJ dysfunction and to assess the impact of gender and age on the occurrence of these manifestations. 144 subjects with clinical diagnosis of TMJ dysfunction underwent MRI of both TMJs. Gender and age, presence of clinical symptoms and MRI morphological manifestation (degree of disk displacement with or without reduction, presence of osteoarthritis and presence of effusion) were recorded. We found that MRI morphological manifestations were associated with the presence of symptoms of TMJ dysfunction. Gender did not correlate with MRI findings. Osteoarthritis was more common in older and effusion was more common in the younger population. Our study confirmed the importance of both clinical examination and MRI imaging in the diagnosis of TMJ dysfunction.

Purpose/Objectives: The purpose of the study was to determine whether the morphological MRI manifestations correlate with the signs and symptoms of TMJ dysfunction according to gender and age of the patients.

Methods and Materials: One hundred and forty-four subjects with TMJ dysfunction underwent MRI of both TMJs to establish the presence of disk displacement, osteoarthritis, and effusion. Chi-square test and logistic regression analysis were performed. For the comparison of mean values between samples, t-test was used.

Results: A significant relationship between symptoms and morphological manifestations was found. In the group without reduction there were significant increases in the risk of experiencing symptoms (P = 0.002). Significant correlation between age and osteoarthritis (P = 0.001) and age and effusion (P = 0.022) was found. There was no correlation between gender and morphological manifestations.

Conclusion: MRI morphological manifestations of the TMJ correlate with the presence of symptoms, therefore MRI has a crucial role in the diagnosis of TMJ dysfunction.

SOPS 4.6.
MRI assessment of the temporal layer of bilaminar zone in patients with temporomandibular joint (TMJ) dysfunction.

A. Lo Casto, A. Avarello, F. Di Naro, P. Purpura, G. Valenti, G. La Tona; Palermo/IT

Short Summary: A retrospective assessment of the temporal layer of the bilaminar zone in patients with TMJ dysfunction, studied by MRI, is presented.

Purpose/Objectives: The bilaminar zone of the TMJ extends posteriorly from the posterior band of the disc and forms two layers, the superior or temporal and lower ones. The temporal layer is composed of loose fibro-elastic tissue rich in elastic fibers and attaches to the postglenoid process, medially extended ridge, which is the true posterior boundary of the joint. It remains in contact with the glenoid fossa when the condyle is in a forward position and it is not stretched across the fossa even in anterior disc displacement without reduction. It avoids slipping of the disk while yawning. Rupture of the temporal layer fibers may produce significant disc instability. This finding is not sistematically analysed in the literature. A retrospective assessment of the temporal layer in patients with TMJ dysfunction, studied by MRI, is presented.

Methods and Materials: MRI exams of 40 patients (11 men, 29 women, age range 19-79 years) with TMJ dysfunction were retrospectively reviewed. MRI exams were made on a 1,5 T device, using a dual-surface coil, between 2012 and 2016. Study protocol included 2 mm thick slices with different sequences: oblique coronal and sagittal TSE PD and oblique sagittal STIR sequences in closed mouth position; dynamic oblique sagittal TSE PD sequence in closed mouth position and different degree of mouth opening.

Results: In 38/40 patients anterior disc displacement was observed. Disc displacement was unilateral in 18/40, bilateral in 20/40 patients. The disc was normally positioned in 2/40 patients. In 6/18 patients with unilateral disc displacement the temporal layer was disrupted. In 2 of these patients a disc reduction was observed during mouth opening, in 4 the disc was not recaptured. In 2/20 patients with bilateral disc displacement the temporal layer was disrupted, and the disc was not recaptured during mouth opening.

Conclusion: Rupture of the temporal layer of the bilaminar zone is an indicator of severe TMJ internal derangement. This finding is associated with chronic anterior disc displacement and is well evaluable by MRI.

SOPS 4.7.

Assessment of the diagnostic accuracy of contrast-enhanced CT in the detection of salivary gland and ductal calculi compared to non-contrast CT

Y. Purcell, A. Carroll, R. Kavanagh, A. Cahalane, M. Rafferty, S.G. Khoo, A. Curran, R. Killeen; Dublin/IE

Short Summary: This retrospective study compares the diagnostic accuracy of contrast-enhanced CT (CECT) to non-contrast CT (NCCT) in the diagnosis of salivary stone/duct calculi and found in favour of CECT.

Purpose/Objectives: The aim of this study is to assess the diagnostic accuracy of CECT in the diagnosis of salivary gland/ductal calculi using NCCT as the gold standard.

Methods and Materials: This is a retrospective, case-controlled study of 50 consecutive patients who underwent both NC and CECT in our tertiary referral centre from December 2012 to December 2015 for investigation of salivary gland/ductal calculi. Axial 3 mm slice images were assessed by a fellowship-trained Neuroradiologist and 4th year Radiology Resident in consensus. Coronal and sagittal images were used for problem solving. Initially, a blinded assessment of the CECT was performed. Following a 2-week interval, a blinded assessment of the NCCT was performed. Determination of the presence or absence of a stone was made at each assessment, and if present, the location and size were recorded. Statistical analysis was performed to assess the agreement between the CT protocols and to calculate the sensitivity/specificity of CECT.

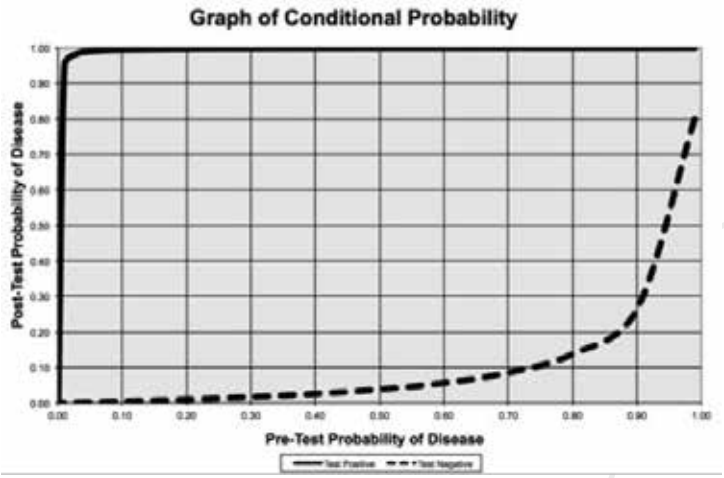

Results: A total of 23 calculi were identified on NCCT in 17 patients. On CECT, 22 calculi were identified; the false negative was a 1mm calculus in the contralateral gland in a patient with a 3 mm calculus in the right parotid gland. All patients with calculi were correctly identified on CECT. This results in a sensitivity of 96% [95% CI 76-100%] of CECT in the detection of salivary gland/duct calculi and a specificity of 100% [95% CI 87-100%]. The positive predictive value of CECT is 100% [95% CI 81-100%] and negative predictive value is 97% [95% CI 83-100%]. The accuracy of CECT in diagnosing the presence or absence of salivary calculi is 98%. If NCCT had been omitted in this study, a mean reduction in DLP of 294.5 +/- 178.1 mGy*cm (effective dose 1.6 mSv using standard neck conversion factor) would have been achieved.

Conclusion: CECT is accurate in the detection of salivary gland/duct calculi. Therefore, it may be possible to omit the non-contrast portion of the study in certain clinical circumstances.

SOPS 4.8.

Ultrasonographic Appearances of Parathyroid Gland in Tertiary Hyperparathyroidism

V. Mingkwansook, C. Buranont; Pathumthani/TH

Short Summary: Tertiary hyperparathyroidisms found in long-standing secondary hyperparathyroidism, resulting in enlarged size and morphologic change of parathyroid glands due to its autonomous hyperfunction. Diagnosis and treatment planning are primarily based on clinical findings and laboratory results. Parathyroidectomy is a surgical procedure for decreased parathyroid hormone levels in patient refractory to medication. Ultrasound (US) could detect abnormal hyperplastic parathyroid glands and facilitate pre-operative planning. The goal of this study is to describe the US appearances of hyperplastic parathyroid glands in tertiary hyperparathyroidism. Our results found that most of parathyroid glands appear as well-defined hypoechoic nodules with peripheral vascularity, similar to those seen in secondary hyperparathyroidism.

Purpose/Objectives: To describe the US findings of parathyroid gland hyperplasia in ESRD patients with tertiary hyperparathyroidism

Methods and Materials: The subject included in the study must had a diagnosis of tertiary hyperparathyroidism with available US of parathyroid glands performed between May 2009 and Jan 2015. All of the subjects must subsequently undergone parathyroidectomy with pathologic confirmation. US findings were retrospectively reviewed by two neuroradiologists. The collecting data included: location, size, echogeniticity, surface, margin, vascularization, cystic changes and intralesional calcification.

Results: There were 28 patients with tertiary hyperparathyroidism who had preoperative US and pathologic confirmation. Time interval between US and parathyroidectomy were 1-9 months. The most common US features were smooth (72.5%), well-defined (100%), hypoechoic (79.3%) nodule with peripheral vascularity (57%) similar to the findings seen on secondary hyperparathyroidism. The size of hyperplastic parathyroid gland ranged from 0.6-3.5 cm (average size 1.3 cm) which is more than that were reported in secondary hyperparathyroidism. The most common location was inferior to the thyroid gland (34.4% on the right size and 22.4% on the left side). Internal cystic changes and calcification were found in 6.9% and 1.7% of the cases, respectively.

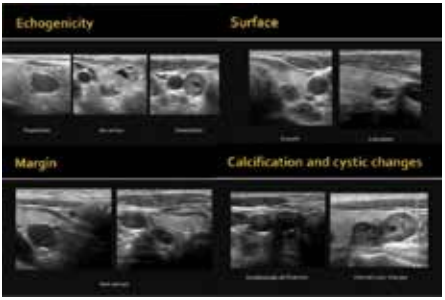

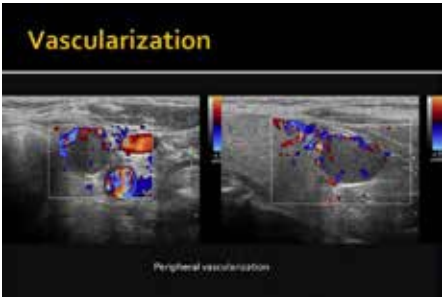

Conclusion: US appearance of tertiary hyperparathyroidism were similar to those found in secondary hyperparathyroidism except the larger average size. This is likely due to tertiary hyperparathyroidism is the long-standing, overt and more severe form comparing to the secondary hyperparathyroidism. US plays a role in confirmation and localization of the enlarged parathyroid glands. Familiarity of these typical appearances could help radiologist detect the hyperplastic gland confidently.

SOPS 4.9.

High resolution ultrasound of the larynx: Imaging technique, normal anatomy and spectrum of disease

S. Jawad, S. Rice, S. Otero, S. Morley, T. Beale; London/UK

Short Summary: We discuss the anatomy, technique and applications of laryngeal ultrasound.

Learning Objectives:

- To revise laryngeal anatomy and describe normal laryngeal appearances on ultrasound.
- To describe optimal ultrasound technique for visualisation of the laryngeal contents as well as the technique for dynamic visualisation of the vocal cord movement.
- To characterise the typical ultrasound appearances of laryngeal malignancy and highlight the important relationship of these to the paraglottic fat and the laryngeal cartilage.
- To characterise how common benign laryngeal conditions appear ultrasonographically.

Background: Ultrasonography is a frequently used imaging technique for the evaluation of head and neck pathology but is scarcely used by radiologists as an imaging modality for the evaluation of the larynx.

Most of the laryngeal contents, even in a heavily calcified larynx, are assessable by high-resolution ultrasound, as the thyrohyoid and cricothyroid membranes are suitable sites for ultrasound transmission.

Ultrasound provides both high resolution and real time imaging and we hope to demonstrate why it is a powerful imaging modality for the diagnosis of benign and malignant laryngeal diseases.

Imaging Findings or Procedure Details: The examination of the larynx should be performed using high-frequency (7-18 MHz) linear and occasionally sector (6.5MHz) transducers, in order to obtain high-resolution images. A pictorial presentation of the technique of laryngeal scanning will be presented.

On ultrasound, laryngeal carcinoma can easily be diagnosed since it appears hypo-echoic. Subtle cartilage invasion is seen by the disappearance of the inner cartilage cortex. Tumoral extension through the cartilage is present when the inner and outer cortex is destroyed by the hypo-echoic lesion.

Ultrasound is useful in diagnosing benign pathology such as: vallecular cysts, thyroglossal cysts, laryngoceles, vocal cord nodules, polyps and cysts, benign cartilage pathology and radiation induced change.

Other important uses include assessment of vocal cord movement and of tracheal stent position and/or complications.

Conclusion: Ultrasonography provides high resolution images and it is a powerful imaging modality for the diagnosis of malignant and several benign diseases.

It has the advantage of being cheap, non-invasive, radiation-free, of higher resolution than cross sectional imaging and suitable for many patients with laryngeal diseases, who have difficulty keeping still during CT or MR acquisition.

SS 6.1.
Case based learning with the expert

I. Schmalfuss, Gainesville/US

Short Summary: The case based learning session will focus on commonly missed pathologies, areas of abnormalities that are often overlooked, interpretational challenges as well as technical pitfalls potentially leading to an incorrect diagnosis. Imaging clues will be discussed to avoid interpretational errors. In addition, guidance will be provided on how to broaden the radiologists search pattern to avoid observational errors.

RC 2.1.
Laryngeal trauma

R. Kohler, Sion/CH

Short Summary: Laryngeal trauma is an infrequent condition secondary to a variety of mechanisms such as direct blow, open trauma, intubation or sneezing. It is however an emergency as it may have potential life-threatening consequences in case of closing of the airway due to hematoma and displaced cartilages as well as frequent associated injuries (vessels, face, cervical spine). Schaefer's classification is clinical and includes hematoma, mucosal disruption, oedema and cartilage fractures; it guides the ENT for the treatment. As endoscopy is able to depict only superficial lesions, imaging is required in case of suspicion of laryngeal trauma. CT is the best technique owing to its accessibility and because it allows the synchronous evaluation of the rest of the body. It is able to depict the soft tissue injuries (hematoma, emphysema, stenosis of the airway) as well as cartilage injuries like fractures, disruptions and displacements of the thyroid cartilage, cricoid cartilage and hyoid bone as well as (sub)luxation of the cricoarytenoid joint. Oblique multiplanar reconstructions, maximum intensity projections, three-dimensional reconstructions and virtual endoscopy are of valuable help for the radiological diagnosis and are also useful for the ENT to decide the treatment (conservative or surgical). There is no consensus about intravenous injection of iodine contrast medium, however it is helpful for the detection of vascular injuries and soft tissue anomalies. MRI is a second line examination mainly used in young patients with hyaline cartilages. Finally, long-term sequelae like cartilage deformation, pseudarthrosis and subglottic stenosis may develop.

Take Home Points:

1. Although rare, laryngeal trauma is a potential life-threatening condition.
2. Fractures and displacements of laryngeal cartilages are the major traumatic lesions of the larynx that may need surgical treatment.
3. CT is the main imaging technique for the evaluation of patients with suspicion of laryngeal trauma and oblique MPRs, MIPs, 3D reconstructions and virtual endoscopy are a useful adjunct.

RC 2.2.
Trauma of the skull base

E. Loney, Darlington/UK

Short Summary: The skull base can at first appear complex but in fact can be simply viewed as having endo- and exo-cranial surfaces. The endocranial surface can be subdivided into 9 regions; right, left and central, each having anterior, middle and posterior components. The exocranial surface is more easily categorised by the bones forming it.

In general, the skull base is extremely 'tough' and requires significant force to injure it. There are however 'weakspots' that are more prone to damage, particularly the cribriform plate and tegmen tympani.

This presentation will consider the anatomy of the skull base, its subdivisions and the types of trauma that may affect it. The amount of force necessary to fracture the skull base means that disruption is often associated with facial and intracranial injuries, and is rarely an isolated event. Fracture patterns and potential complications will be discussed with particular emphasis on the best radiological techniques to make often difficult diagnoses.

Take Home Points:

1. The skull base is tough- it takes a lot of force to damage it and injuries are rarely isolated. Always look for associated intracranial and extracranial pathology.
2. Consider the anatomy and compartment(s) affected when looking at trauma scans. Always check relevant 'weakspots' for injury.
3. Think about the mechanism of trauma- this will affect the pattern of bony injury and associated soft tissue damage.

RC 2.3.
Orbital trauma

P. de Graaf, Amsterdam/NL

Short Summary: Orbital injury is common among trauma patients. Subsequent traumatic ocular and optic nerve injury are a significant cause of blindness and visual deficits. Assessing the full extent of traumatic orbital injuries is an important challenge for radiologists, especially when the orbital injury is associated with injuries involving multiple organs. However, in the acute trauma setting, clinical evaluation of the orbit and globe may be difficult in the presence of periorbital soft-tissue swelling and other associated injuries, and the radiologists may be the first to identify sight-threatening problems on imaging. Full awareness of the imaging features of orbital trauma, and the potential complications of damage to the eye and optic nerve, makes it possible to diagnose sight-threatening problems before permanent visual loss might occur. The imaging features of orbital and ocular trauma will be reviewed with a specific focus on the associated morbidity.

Take Home Points:

- Know the patterns of orbital fractures and the possible complications of damage to the intra-orbital structures (eye, extra-ocular muscles, cranial nerves).
- Recognise the imaging features that allows the radiologist to diagnose traumatic orbital and ocular pathologies that cause long-term visual morbidity (blindness, visual deficits or diplopia)

SS 7.1.
Dual energy CT: Applications in Head and Neck radiology
L. Jacobi-Postma, Maastricht/NL

Short Summary: The choice of imaging modality and protocol is tailored to the area and tissues of interest and questions to be answered. CT, MRI and ultrasound are in the last decade completed by PET-CT, advanced MR-imaging, and PET-MR.

The development of CT has led to an increase of spatial and temporal resolution and (re-) expanded indications in general. Dual-energy CT (DE-CT) has been added to the advanced CT techniques in the first decade of this millennium.

DE-CT uses two X-ray spectra instead of one to create two CT-datasets. This can be achieved in different ways: Two simultaneous operating tubes with different kVp's, fast kV-switching, dual-layer detector technology or scanning twice.

By applying two different energy spectra, characterization of materials is feasible. In this way one can differentiate materials and calculate spectral curves, mono-energetic images, effective electron density and effective atomic numbers.

The applications in head and neck imaging are expanding, and its value is increasingly recognized.

With virtual mono-energetic reconstruction, an image dataset is calculated as if it was scanned using a mono-energetic energy. By choosing a virtual lower energy, the contrast in the image is increased.By approaching the k-edge of iodine, the attenuation of iodine is augmented. In this way enhancing tissues are more easily depicted, the detection and delineation of pathology, like abscesses and head and neck squamous cell carcinoma (SCC), is improved. Reconstructions at higher virtual mono-energetic energies enable reduction of dental metallic artifacts, the CNR is decreased and SNR is increased.

By characterization of iodine, iodine maps, fusion images and iodine concentration can be calculated. These can be used to discriminate normal, inflammatory and metastatic lymph nodes or head neck SCC. Detection of cartilage invasion in laryngeal SCC can be improved with iodine maps, fusion images and mono-energetic reconstructions at lower keV.

Bone characterization is used in bone-removal in head-neck-CTA.

The use of virtual non-contrast images, calculated from a contrast-enhanced dataset, makes it possible to abstain a real non-contrast CT scan, e.g. in parathyroid multi-phase scanning.

Take Home Points:

DE-CT allows for multiple reconstructions from one single scan.

DE-CT can aid in detection, delineation and discrimination of head and neck pathology

SS 7.2.
CT perfusion: Will it replace MR perfusion?
A. Trojanowska, Lublin/PL

Short Summary: Computed tomography perfusion (CTP) is a technique that allows quick qualitative and quantitative evaluation of tissue perfusion by generating maps of cerebral blood flow (BF), blood volume (BV), mean transit time (MTT) and permeability surface (PS). Perfusion CT has been found to be useful for non-invasive diagnosis of many diseases like cerebral ischemia and infarction, tumoral neo-angiogenesis, malignant infiltration of surrounding tissues, differentiation between malignant and benign processes and for tumour response to radio- and chemotherapeutic treatment. Recent studies, based on ultrasound imaging of the primary tumour vascularisation, showed that CTP parameters may provide information on vascularisation of lymph nodes and tissues and may reflect angiogenic activity, helping to understand the changes occurring when malignant process occurs. CTP has been found especially useful in monitoring the efectiveness of non-surgical treatment and early treatment response in case of squamous cell cancer. This information will probably allow to plan the appropriate therapy and swich to more effective treatment option in case of non-responding tumors.

SS 7.3.
CBCT: Dental and maxillofacial imaging
R. Saat, Helsinki/FI

Short Summary: Cone beam computed tomography (CBCT) is an imaging technique that utilises cone-shaped x-ray beam and flat-panel detectors together with computational image reconstruction, yielding 3D imaging data of limited volumes with high spatial resolution. The method is especially well suited for hard tissue imaging and, hence, is increasingly popular in dentomaxillofacial radiology.

This lecture will mainly focus on clinical use of dentomaxillofacial CBCT.

Advantages and disadvantages of CBCT in comparison with MDCT and radiography will be discussed.

Recent literature and current guidelines for clinical use of CBCT in dental practice will be reviewed.

The leading applications of CBCT, such as dental implant or mandibular third molar extraction planning, will be discussed in little more detail.

Few other clinical examples of CBCT's benefits will be provided together with hints for reading dental (CB)CT scans for those who are not too familiar with oral health or dental imaging problems.

Take Home Points:

- In comparison with two-dimensional radiography, CBCT can provide increased geometrical accuracy and clinically useful 3D information. However, its use should be limited to selected indications.
- There is a remarkable variation between technical parameters of different scanners that has direct impact on their clinical performance.
- One of the undisputable advantages of CBCT over MDCT is its lower cost. The effective radiation dose from CBCT scans varies widely according to the equipment and settings used, but notable reduction in dose can be achieved with small fields of view.
- In CBCT reports, detailed anatomical and pathological information should be provided not only on the tooth in question, but also on its neighbouring teeth and adjacent bone.

SS 8.1.
DWI and DCE MRI

R. Hermans, Leuven/BE

Short Summary: CT and MRI are well established methods in the initial diagnostic evaluation of head and neck malignancy, and are also used for treatment monitoring and follow-up.

The characterisation of neck lymph nodes may be difficult with anatomy-based imaging methods. High sensitivities and specificities were reported using diffusion-weighted MRI (DWI), mainly due to improved detection of subcentimetric nodal metastases. Differentiation of treatment induced tissue changes and persistent or recurrent cancer, is another topic in which DWI may be helpful. Also, studies investigating the role of DWI as prognostic tool during, and very early after treatment, are ongoing. Preliminary results are encouraging, and if confirmed, tailoring treatment according to the very early individual response, as seen on DWI, may become feasible. Difficulties related with the routine use of DWI are the current lack of standardization across centers, concerns about reproducibility, availability of only few validation studies, and last but not least the time-consuming analysis of the images.

Dynamic contrast-enhanced (DCE) MRI allows non-invasive assessment of tissue blood flow during bolus administration of a contrast agent. Various methods are being used to analyse such images. Potential applications include tumor identification, tumor characterisation and monitoring treatment response. Difficulties related with the routine clinical use of DCE-MRI are similar as for DWI.

Take Home Points:

CT and MRI are well established methods in the evaluation of head and neck cancer

DWI and DCE-MRI can serve as non-invasive biomarkers in a research setting

DWI and DCE-MRI may be of complementary value to the routine spin-echo sequences in the clinical setting

SS 8.2.
PET MRI
M. Becker, Geneva/CH

Short Summary: PET/CT and MRI with diffusion-weighted imaging (DWI) are complementary and reliable techniques for the assessment and staging of head and neck tumors. The recent implementation of hybrid MR/PET systems in clinical settings is promising as morphologic, functional and molecular information can be obtained in a single examination.

This lecture focuses on clinical applications of MR/PET in head and neck tumors with special emphasis on squamous cell carcinoma. The principles of MR/PET data fusion are reviewed, including current evidence regarding clinical feasibility, image quality, optimized imaging protocols and quantification with MRI based attenuation algorithms. Current knowledge regarding the diagnostic performance of MR/PET in the head and neck is discussed and typical tumour manifestations are presented. The appearance of primary and recurrent squamous cell cancers, lymph node metastases and distant metastases on MR/PET, as well as the value of multiparametric imaging are summarized. The variable appearance of functional phenomena mimicking disease, as well as potential pitfalls of image interpretation due to morphological or functional post-treatment changes are addressed. Illustrative cases of concordant and discrepant multiparametric evaluations are equally discussed as well as the dilemma of how to deal with discrepant multiparametric data.

Take Home Points: MR/PET is still a reserach tool in head and neck oncology with the advantage of combining high-resolution anatomic, morphologic and functional information in a single examination.

Although SUV values measured on MR/PET are underestimated in comparison to PET/CT, MR/PET detects focal FDG uptake equally well as PET/CT.

The complementarity between diffusion weighted imaging and PET is especially valuable for the assessment of the treated head and neck.

SS 8.3.
Sentinel lymph node imaging in the head and neck: principles and clinical applications
R. de Bree, Utrecht/NL

Short Summary: Oral cancer is one of the most common head and neck malignancies. As lymph node metastases are one of the most important prognostic factors an elective neck dissection (END) has been widely performed for accurate staging of the cervical lymph nodes. However, up to 75% of patients are overtreated and may suffer from side effects of END.

To avoid unneccessary neck dissections sentinel lymph node biopsy (SLNB) as an alternative for neck staging in clinically node negative patients with oral cancer have been introduced. A high detection rate, sensitivity (>90%) and low false negative rate (<5%) of SLNB was demonstrated in multicenter studies. SLNB is nowadays routinely used in many head and neck centers. SLNB for early oral cancer is incorporated in the national guidelines of the USA,

UK and The Netherlands. However, due to the complex lymphatic drainage and close vicinity of the injection site SLNB in head and neck is challenging, particularly when the primary tumor is located in the floor of mouth. The development of new tracers and technologies might facilitate the intraoperative detection of SLNs and improve results of SLNB.

Take Home Points:

The sentinel node biopsy procedure is a highly accurate staging technique for patients with early oral cancer and a clinically negative neck.

Sentinel node biopsy in floor of mouth cancer is challanging and can be improved by new tracers, camera systems and probes.

NHS 3.1.
From photon to proton therapy: Implications for imaging

A.D. Jensen, Bern/CH

Short Summary: The main technological advances within past decades have increased the radiotherapy therapeutic window by increasing dose conformity and thereby reducing doses to adjacent critical structures. This is especially true for charged particle therapy (protons or heavy ions): as opposed to photons, charged particles have a finite range in tissue which is dependent on the particle's kinetic energy. Protons and heavy ions loose most of their energy at the end of their path resulting in extremely steep dose gradients. Consequently, radiotherapy with charged particles is used to treat tumours at challenging anatomical sites such as the head and neck and skull base. It is established for the treatment of rare and radio-resistant tumours such as chordoma (CO), chondrosarcoma (CS), and malignant salivary gland tumours (MSGT). In addition to dosimetric advantages in charged particle radiotherapy, heavy ions additionally offer the benefit of increased biological effectiveness and relative independence of the oxygen effect.

As treatment precision increases with the aim of dose escalation, this calls for more precise tumour delineation and target volume definition but also for a close monitoring throughout treatment and follow-up.

Especially in MSGTs, perineural spread is common: undetected it is a frequent cause of locoregional relapse at the skull base and difficult to treat. High-resolution imaging of potential areas and early detection of perineural spread is therefore of utmost importance. Also, tumour response following high-dose radiotherapy may differ: while MSGTs, CO, and CS may need years to measurably respond according to RECIST functional changes may be detected much earlier.

Last but not least, detection of radiogenic normal tissue changes and differentiation from local relapse is challenging and needs interdisciplinary efforts to improve diagnosis.

Take Home Points: Particle therapy is a new treatment technique for malignant tumours of the head and neck with enormous potential in treating radio-resistant and hypoxic tumours but also in reducing late sequelae in standard HNSCC. With increasingly precise target volume definition, there is increasing demand for high-resolution and functional imaging for treatment planning and adaptation. Functional imaging techniques may be increasingly required for response assessment and differentiation of local relapse vs radiogenic normal tissue changes.

RC 3.1.
Digital supported interactive learning: anatomy based approach of spread of diseases: oral cavity and floor of the mouth

A. van der Gijp F. Pameijer, Utrecht/NL

Short Summary: The oral cavity contains many anatomical structures that are in close proximity of each other and is therefore challenging to assess. A good understanding of the relevant anatomy and the various spaces is required, as well as knowledge of the spread of disease in this area of the head and neck. In this workshop, we use a digital application with annotated CT and MR scans to demonstrate the three-dimensional relations of the anatomical structures. We selected several anatomical structures of the oral cavity that are important landmarks and discuss related pathology. We focus on three subsites of the oral cavity: (1) the tongue, (2) the floor of the mouth and (3) the root of tongue. Important anatomical structures of the tongue are the extrinsic tongue muscles, due to their involvement in the TNM staging of oral cavity tumors. In the floor of the mouth, the mylohyoid muscle plays an important role in separating the sublingual from the submandibular space. Understanding the specific anatomy of the mylohyoid muscle improves understanding of related diseases, such as diving/plunging ranulas. The root of tongue is an important subregion of the oral cavity which should not be confounded with the base of tongue (i.e. a subsite of the oropharynx). The root of tongue consists of the lingual septum and genioglossus and geniohyoid (extrinsic tongue) muscles. In the root of tongue, thyroglossal duct cysts and lingual thyroid may occur, because in embryology, the thyroglossal duct traverses the root of the tongue.

Take Home Points:

For remembering muscle anatomy in the oral cavity: connect the dots

The sublingual and submandibular space communicate through the free edge of the mylohyoid muscle

Thyroglossal duct cysts and lingual thyroid can occur in the root of the tongue

RC 3.2.
The normal and diseased oropharynx
M. Lemmerling, Gent/BE

Short Summary: The oropharynx is the portion of the pharynx posterior to the oral cavity, superior to the hypopharynx, and inferior to the nasopharynx. The superior and middle pharyngeal constrictor muscles form the lateral and posterior walls of the oropharynx, which contains the palatine tonsils. These lymphoid aggregates are covered by non-keratinised squamous stratified epithelium. This epithelium continues down into deep crypts, in which tonsilloliths can develop, sometimes causing halitosis. The pharyngeal tonsils contribute to Waldeyer 's ring, the first organ in the lymphatic system to analyze and react to airborne and alimentary antigenic stimulation. In case of failure, disease develops, most frequently of infectious or neoplastic origin. Tonsillitis can, if not or partially treated, develop to peritonsillitis and peritonsillar abscess. Squamous cell carcinoma is the most frequent malignancy seen in the oropharynx, and is mostly related to alcohol abuse and excessive smoking, with HPV type 16 viral infection coming in recently as a new important risk factor. Tonsillar carcinoma, tongue base carcinoma, and posterior pharyngeal wall carcinoma behave slightly differently, as seen on imaging studies. Posterior pharyngeal wall tumors, as suspected on inspection by the ENT surgeon, can be mimicked by large retropharyngeal lymph nodes or osteophytes, or by the retropharyngeal course of the internal carotid artery. Other less frequent oropharyngeal tumors are lymphoma (majority extranodal NHL), and rarely salivary gland tumors. H&N lymphomas have a relatively specific 'imaging behavior', enhancing the importance of the radiologic report. In most other circumstances the function of the radiologist in reporting oropharyngeal disease is not specifically diagnostic, but is rather important in view of description of disease extent, to help guiding surgical intervention, or narrow down the differential diagnosis.

Take Home Points:

Oropharyngeal diseae is most frequently of infectious or neoplastic origin.

Squamous cell carcinoma and lymphoma are the most frequent oropharyngeal malignancies

RC 4.1.
Neoplasms of the salivary glands
M. de Win, Amsterdam/NL

Short Summary: Neoplasms of the salivary gland are uncommon and mostly benign. The tumours mainly affect the major salivary glands, but they can also originate from the minor salivary glands. About 80% percent of the tumours occur in the parotid, of which 80% are benign. In the smaller salivary glands the malignancy rate is higher.

Most are epithelial lesions. The benign pleomorphic adenoma is most common, it typically is lobulated, T2 hyperintens, with moderate contrast enhancement. Whartin's tumour (adenolymphoma) occurs in the parotid gland, can be bilateral and is related to cigarette smoking. They commonly show cystic areas and no contrast enhancement, but they can show FDG uptake and diffusion restriction, mimicking malignancy.

Malignant epithelial tumours include mucoepidermoid carcinoma, adenoid cystic carcinoma, adenocarcinoma, carcinoma ex-pleomorphic adenoma and squamous cell carcinoma.
The mucoepidermoid is the most common salivary gland malignancy. They are ill defined, heterogeneous, with low signal on all MRI sequences and low ADC values. Adenoid cystic carcinoma is the most common malignant tumour in the submandibular and sublingual glands. They tend to spread by perineural invasion. Malignant mixed tumours can develop from pleomorphic adenomas (carcinomas ex-pleiomorphic adenomas). On MRI they show low signal intensities on T1 and T2 and diffusion restriction.

Non-epithelial tumours of the salivary gland include lipoma, haemangioma, neurogenic, malignant lymphoma, sarcoma.

Imaging is important for preoperative planning to detect origin, multifocality, local extension, invasion and nature of the lesion. MRI is first choice and diffusion MRI should be part of the standard protocol. Malignant lesions mostly show low T2 signal, ill-defined margins and diffusion restriction. DCE-MRI can be used to further characterize the tumour. However, overlap with benign and malignant lesions occur.

Take Home Points:

- Salivary gland tumours are rare and are benign. The smaller the salivary gland the higher the rate of malignancy
- The main aim of preoperative imaging is detect origin, multifocality, local extension, invasion and nature of the lesion. MRI is first choice.
- DWI and DCE MRI are useful techniques in characterising salivary gland tumours

References: Freling et al 2016, Aghaghazvini et al 2015, Lam et al 2014, Yabuuchi et al 2008, Madani et al 2006

RC 4.2.
Diagnosis and staging of salivary gland tumors

N. Freling, Amsterdam/NL

Short Summary: After curative treatment for Highl-grade malignant Salivary Gland Tumours (HGMSGT) clinical examination is impeded by altered anatomy and fibrosis. Recurrences, especially within the deep compartments of the face, and perineural spread may go unnoticed clinically at its earliest stage. Seventy percent of recurrences of HGMSGT are seen within 3 years of treatment. The efforts in surveillance should focus in particular on recurrences whose detection may have clinical consequences, i.e. that are still treatable with a curative intention.

MRI is the most appropriate imaging technique for precise local mapping of primary malignant salivary tumours. Although new developments such as diffusion (DWI/ADC) and perfusion (DCE-MRI / IVIM) MRI suggest better differentiation among tumour types, the reported numbers are too low to draw firm conclusions. US with FNAC is recommended for assessing the nature of a primary salivary gland tumour and N-staging the neck.

Because most distant metastases do occur in the lungs, chest-CT may be considered. A base-line MRI of the head and neck is recommended in patients with high-grade malignant tumours in whom local recurrence rates are high. In patients with loco-regional recurrent disease, MRI, if possible combined with US-guided FNAC, is the preferred imaging technique to direct treatment strategies. In case of distant metastases during follow-up, chest-CT or symptom-related imaging is recommended. MRI of the head and neck in combination with CECT of the chest and abdomen plays an important role for evaluation of experimental chemotherapy in patients with advanced primary salivary gland tumours or recurrent disease.

Take Home Points:

MRI is the most appropriate imaging technique to locate a salivary gland tumour, to assess its extension and to demonstrate perineural spread at presentation and during follow-up.

DWI/ADC may help to identify recurrent disease

A base-line MRI study after completion of therapy is recommended for high-grade malignant tumours

Imaging during follow-up of HGMSGT is mainly directed by new cancer treatment protocols and includes routine chest-CT and MRI of the H&N.

Abstracts appear as submitted to the online submission system and have not been checked for correctness and completeness.

POSTERS

Educational Posters

EP-01 The non-experts survival guide on surgery for carcinoma of the oral tongue
K.A. Eley[1], S. Watt-Smith[2]; [1]Cambridge/GB, [2]London/UK

EP-02 Imaging in Sensorineural Hearing Loss
C. McArthur, D. Rawlings; Kilmarnock/UK

EP-03 Pictorial Review of Muscular Denervation Changes due to Cranial Nerve Pathology
B. de Kok, C. Tolman; The Hague/NL

EP-04 Nasal Paraganglioma: Pictorial Differential Diagnosis from a Radiologic and Pathologic Perspective
C. Tolman; The Hague/NL

EP-05 Peripheral vertigo on imaging
H. Lindmae, H.E. Westerlaan; Groningen/NL

EP-06 Benign cystic neck masses: embryology and imaging findings
K. van Langevelde, B. Verbist; Leiden/NL

EP-07 Lemierre's Syndrome: Case Based Diagnostic Approach
E. Civgin, U. Toprak, I.S. Parlak, H. Özer; Ankara/TR

EP-08 Renal cell cancer metastasis to the thyroid gland: a case report demonstrating a new thyroid ultrasound sign
S. Colley, A. Aziz, E. McLoughlin; Birmingham/UK

EP-09 CT Findings in Hoarseness and/or Vocal Cord Paralysis
M. Shahid, B. Adams, S. Karthik; Leeds/UK

EP-10 Spontaneous Bilateral Sternocleidomastoid Haematomas of unknown aetiology, a rare presentation
M. El Farargy, M. Selmi, M. Natarajan; Manchester/UK

EP-11 Tongue Tumor - Make it Easier Focusing on Where to Look for to Get the Right Staging!
L. Fernandes, I. Leite, M. Roque, S. Palma, P. Pereira, A.R. Santos; Lisbon/PT

EP-12 Parapharyngeal Space Lesions that are Hypointense on T2 Weighted Sequences: A Local Review
E. Vassallo, M. Ravanelli, I. Zorza, V. Mazza, D. Farina, R. Maroldi; Brescia/IT

EP-13 Imaging and Histopathological Findings in Lesions Involving the Skull Base
D. Haba, G. Dumitrescu, A. Dumitrescu, R. Vreme, M. Haba, A. Sava, D. Turliuc, B. Iliescu, V. Costan; Iasi/RO

EP-14 Juvenile (particularly) aggressive ossifying fibroma, in a less typical localization
M. Veiga, M. Diogo, J. Ramalho, C. Pinheiro, C. Perry da Câmara, R. Carranca; Lisbon/PT

EP-15 "Pyriform Aperture Stenosis - a rare, but fatal, cause of nasal obstruction in infants"
C. Pinheiro, M. Veiga, M. Diogo, J. Ramalho, M. Ferreira, C. Conceição; Lisbon/PT

EP-16 Imaging of congenital lesions in the nasofrontal region
S. Pieters-Kan, H.E. Westerlaan; Groningen/NL

EP-17 Anatomy, anatomical variations and pathologies of the sphenoid sinuses
F. Albert, S. Greschus; Bonn/DE

EP-18 Holes in the skull - The differential diagnosis of lytic skull lesions
M. Veiga, M. Diogo, J. Ramalho, C. Pinheiro, C. Perry da Câmara, C. Conceição; Lisbon/PT

EP-19 Temporomandibular Joint – What to look for?
J. Lieb; Basel/CH

EP-20 Ultrasound assessment of the oral cavity and oropharynx: techniques and applications
S. Jawad, S. Otero, S. Morley, T. Beale; London/UK

EP-21 High resolution ultrasound of the larynx: Imaging technique, normal anatomy and spectrum of disease
S. Jawad, S. Rice, S. Otero, S. Morley, T. Beale; London/UK

EP-22 Typical and atypical CT features of sinus fungus ball: a retrospective analysis of 83 consecutive patients with radiologic pathology correlation
C. Tarantino, F. D'Amore, F. Pagella, A. Pusateri, G. Giustiniano, G. Di Giulio; Pavia/IT

Scientific Posters

SP-01 Oral floor and neck muscles ultrasound anatomy in Polish and Turkish young adults
I. Rozylo-Kalinowska[1], N. Yetimoglu Ozdil[2], P. Kalinowski[1], K. Orhan[2]; [1]Lublin/PL, [2]Ankara/TR

SP-02 Tonsilloliths on dental panoramic radiographs - prevalence in a sample of Polish population
I. Rozylo-Kalinowska, K. Denkiewicz; Lublin/PL

SP-03 Suprahyoid Airway Volume Analysis in Dentofacial Pattern Discrepancy by Using CBCT: A Longitudinal Case Study
A. Mohi, S. Yalcinkaya; Istanbul/TR

SP-04 Ultrasonographic Appearances of Parathyroid Gland in Tertiary Hyperparathyroidism
V. Mingkwansook, C. Buranont; Pathumthani/TH

SP-06 Mandible Radiographs: a retrospective study in a district general hospital without direct access to orthopantogram – Are oblique lateral and PA radiographs sufficient?
K.A. Eley; Cambridge/UK

SP-07 The diagnostic accuracy of non-imaging screening protocols for vestibular schwannoma: a diagnostic review and meta-analysis
M. Hentschel, M. Scholte, S. Steens, H. Kunst, M. Rovers; Nijmegen/NL

SP-08 Tortuosity of the internal carotid artery is associated with vocal cord paralysis
J. Maier; Køge/DK

SP-09 CT Imaging Findings of Laryngeal Amyloidosis
L.W. Goh, J. Shenoy, T.Y. Tan; Singapore/SG

SP-10 The added value of SPECT-CT for identification of sentinel lymph nodes in early stage oral cancer
I. den Toom[1], A. van Schie[2], S. van Weert[2], O.S. Hoekstra[2], K.H. Karagozoglu[2], E. Bloemena[2], R. de Bree[1]; [1]Utrecht/NL, [2]Amsterdam/NL

SP-11 MR Imaging of Carcinoma Tongue - Prospective evaluation
S. Jayasankaran, P. G Chelakot, M. K, K.K. Thankappan, S. Moorthy; Kochi/IN

SP-12 Preoperative Protective Stenting in Paraganglioma
F. Götz, O. Majdani, T. Lenarz, H. Lanfermann, A. Giesemann; Hannover/DE

SP-13 Late Contrast-Enhancement of the IAC-Fundus
F. Götz, P. Dellani, H. Schmitt, O. Majdani, T. Lenarz, H. Lanfermann, A. Giesemann; Hannover/DE

SP-14 Are variations and infundibular tract length a myth in the development of maxillary sinusitis? Is mucociliary function failure solely to be blamed?
L. Pasaoglu, U. Toprak, E. Üstüner, M.S. Besler; Ankara/TR

SP-15 Using diffusion-weighted MRI to assess treatment response in Necrotizing Otitis Externa: Initial experience with case series
D. St Leger, A. Singh, R. Lingam; London/UK

SP-16 Visibility of the discomallear ligament on high-resolution computed tomography of the temporal bone
E. Arkink[1], B. Verbist[1, 2]; [1]Leiden/NL, [2]Nijmegen/NL

SP-17 Multiplanar evaluation of ameloblastoma for locularity and solid tumor nodule: the impact on surrounding structures
J.-E. Kim, K.-H. Huh, J.-B. Cho, G.-D. Jo; Seoul/KR

SP-18 The Appearance of The Infraorbital Canal and Infraorbital Ethmoid (Haller's) Cells On Panoramic Radiography of Edentulous Patients
E. Yesilova, I.S. Bayrakdar; Eskisehir/TR

SP-19 PET CT in the assessment of Head and Neck cancer post treatment
L.J. Steinberg, S. Mak, S. Bonington; Qj/UK

SP-20 Evaluation of cholesteatoma recurrence using diffusion-weight MR imaging versus second look mastoidectomy
M. Daoud, C. Tettey, R. Capper, J. Dugar, N. Dugar; Doncaster/UK

SP-21 How can Fusion of CT/diffusion weighted MRI images help in evaluating cholesteatoma
A. Hall, D. St Leger, A. Singh, R. Lingam; London/UK

SP-22 Restriction of mouth opening and neck movement in patients with fibrodysplasia ossificans progressiva: report of two cases with emphasis on MR findings
G.-D. Jo, K.-H. Huh, J.-E. Kim; Seoul/KR

SP-23 Morphometric evaluation of temporal bone using Cone Beam CT
N. Yetimoglu Ozdil, K. Orhan, U. Seki; Ankara/TR

SP-24 Incidence of impacted tooth in Turkish subpopulation: A retrospective study
S. Kalkan, M. Sakir, A. Dumlu; Istanbul/TR

SP-25 Evaluation of the prevalence of maxillary sinus septa in Turkish population using cone-beam computed tomography
M. Sakir, S. Kalkan, A. Dumlu; Istanbul/TR

SP-26 Discerning Ocular Globe Anatomy in clinical Brain MRI Protocol
M. Diogo[1], T. Ferreira[2], C. Conceição[1]; [1]Lisbon/PT, [2]Leiden/NL

SP-27 Adenoid cystic carcinoma of the head and neck region – morphologic characteristics in MRI
S. Greschus, F. Albert; Bonn/DE

SP-28 Evaluation of the Parotid Gland with Ultrasonography in Patients with Type 2 Diabetes
T. Cimen, F. Yasar; Konya/TR

SP-29 CT findings in non-bisphosphonate drug related osteonecrosis of the jaws (DRONJ)
A. Lo Casto[1], V. Fusco[2], F. Di Naro[1], L. Benzi[2], C. Lunetta[1], G. La Tona[1]; [1]Palermo/IT, [2]Alessandria/IT

SP-30 Setting up a parathyroid multi-disciplinary team meeting; one year's experience, outcomes and learning points
S. Hancox, J. Sinnott, P. Kirkland, D. Lipscomb, E. Owens, D. Howlett; Ud/UK

SP-31 Interobserver agreement in the detection of recurrent HNSCC using diffusion weighted MRI
B. Peltenburg, J.P. Driessen, M.E.P. Philippens, F. Pameijer, I. Stegeman, L. Janssen, R. de Bree, W. Grolman, C. Terhaard; Utrecht/NL

Poster titles appear as submitted to the electronic poster submission system and have not been checked for correctness and completeness.

POTENTIAL CONFLICT OF INTEREST DISCLOSURE

It is the policy of the European Society of Head and Neck Radiology to ensure balance, independence, objectivity, and scientific rigour in the congress programme. Knowledge of possible relationships with sponsors of any kind is mandatory in order to reinforce the educational and scientific message and to relieve any suspicion of bias.

Any potential conflict of interest involving ESHNR speakers should be made known so that the audience may form their own judgements about the presentation with a full disclosure of the facts.

It is for the audience to determine whether the presenter's external interest may reflect a possible bias in either the work carried out or the conclusions presented.

The individual listed below disclosed the following relationships:

A. Van der Lugt:	Receipt of grants/research supports: GE Healthcare Receipt of honoraria or consultation fees: GE Healthcare
B.M. Verbist:	Research grant for PhD student: Advanced Bionics Travel and speaker reimbursement: Bayer

PRESIDENT & COMMITTEES

Meeting President 2016

B.M. Verbist, Leiden/NL

Local Scientific Committee

J.A. Castelijns, Amsterdam/NL
J.-C. de Groot, Groningen/NL
M. de Win, Amsterdam/NL
N.J.M. Freling, Amsterdam/NL
M. Palm, Maastricht/NL
F.A. Pameijer, Utrecht/NL
S. Steens, Nijmegen/NL
A. van der Lugt, Rotterdam/NL

Local Organizing Committee

N.J.M. Freling, Amsterdam/NL
F.A. Pameijer, Utrecht/NL

Scientific Committee

T. Beale, London/UK
M. Becker, Geneva/CH
K.S.S. Bhatia, Hong Kong/HK
S. Bisdas, London/UK
A. Borges, Lisbon/PT
C. Czerny, Vienna/AT
B. de Foer, Antwerp/BE
P. de Graaf, Amsterdam/NL
F. Dubrulle, Lille/FR
H.B. Eggesbo, Oslo/NO
D. Farina, Brescia/IT
N.J.M. Freling, Amsterdam/NL
D. Haba, Iasi/RO
R. Hermans, Leuven/BE
R. Kohler, Sion/CH
M.G. Mack, Munich/DE
R. Maroldi, Brescia/IT
J. Olliff, Birmingham/UK
S. Petrovic, Nis/RS
S. Robinson, Vienna/AT
A. Trojanowska, Lublin/PL
D.A. Varoquaux, Marseille/FR
B.M. Verbist, Leiden/NL

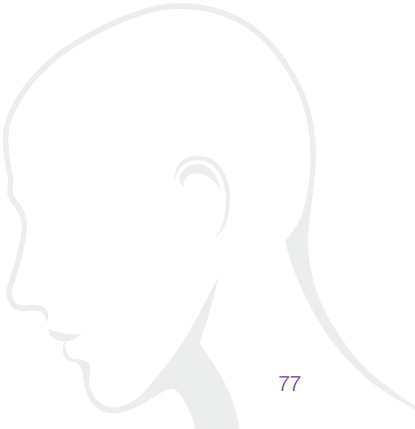

FACULTY

T. Beale, London/UK
M. Becker, Geneva/CH
K.S.S. Bhatia, Hong Kong/HK
S. Bisdas, London/UK
A. Borges, Lisbon/PT
J.W. Casselman, Bruges/BE
J.A. Castelijns, Amsterdam/NL
C. Czerny, Vienna/AT
R. de Bree, Amsterdam/NL
B. de Foer, Antwerp/NL
P. de Graaf, Amsterdam/NL
J.C. de Groot, Groningen/NL
B. de Keizer, Utrecht/NL
M. de Win, Amsterdam/NL
E.E. Deurloo, Amsterdam/NL
F. Dubrulle, Lille/FR
H.B. Eggesbo, Oslo/NO
R. Evans, Wales/UK
D. Farina, Brescia/IT
T.A.G.G. Ferreira, Leiden/NL
N.J.M. Freling, Amsterdam/NL
D. Haba, Iasi/RO
R. Hermans, Leuven/BE
L. Jacobi-Postma, Maastricht/NL
A. Jensen, Bern/CH
S. Kant, Leiden/NL
C. Karaman, Aydin/TR
J. Kievit, Leiden/NL
R. Kohler, Sion/CH
S. Kösling, Halle a. d. Saale/DE
M. Kriek, Leiden/NL
M. Lamers, Groningen/NL
A.P.M. Langeveld, Leiden/NL
M. Lemmerling, Beervelde/BE
E. Loney, Darlington/UK
M.G. Mack, Munich/DE
R. Maroldi, Brescia/IT
P. Nicolai, Brescia/IT
J. Olliff, Birmingham/UK
M. Palm, Maastricht/NL
F.A. Pameijer, Utrecht/NL
S. Petrovic, Nis/RS
R. Rhys, Cardiff/UK
P. Richards, London/UK
S. Robinson, Vienna/AT
R. Saat, Helsinki/FI
I. Schmalfuss, Gainesville/US
B.F. Schuknecht, Zurich/CH
E.V. Sjögren, Leiden/NL
S. Steens, Nijmegen/NL
A. Trojanowska, Lublin/PL
A. van der Gijp, Utrecht/NL
A. van der Lugt, Rotterdam/NL
D.A. Varoquaux, Marseille/FR
B.M. Verbist, Leiden/NL
A.G. Webb, Leiden/NL

WELCOME RECEPTION

Thursday, September 22, 2016

Time: Starting at 17:30 local time
Venue: City Hall, Stadhuisplein 1, 2311 EJ Leiden, The Netherlands
Price: free of charge, registration compulsory

The City Hall is located at the heart of old Leiden. In the 16th century a monumental Renaissance façade was built in front of the medieval town hall. Despite a devastating fire in 1929 this façade is still standing and currently the longest one in the Netherlands. The renowned architect CJ Blaauw rebuilt the city hall with bell tower and part of the new interior was designed by Escher.

We cordially invite you to the ESHNR 2016 Welcome Reception, which starts subsequently to the scientific programme. Snacks and drinks will be served at the City Hall for participants of ESHNR 2016. Take the chance and get in touch with experts and colleagues from Europe and from all over the world.

We are looking forward to seeing you!

ESHNR GALA DINNER

Friday, September 23, 2016

All delegates are invited to round off the congress day at the Hortus Botanicus.

Time: Starting at 18:45 local time
Venue: Hortus Botanicus, Rapenburg 73, 2311 GJ Leiden, The Netherlands
Price: EUR 55.00 per ticket (Please contact the staff at the registration desk). The ticket grants access to the botanical garden during the whole day.

The Hortus Botanicus of Leiden is the oldest botanical garden of the Netherlands and one of the oldest in the world. Behind the academy building of the Leiden University you will discover a green oasis with a large collection of plants native to South-east and East Asia, Southern Europe and South Africa. The Hortus is a haven within the city centre, a historical monument and a meeting place full of character. People come here to relax, enjoy the seasons or to learn more about the diversity of the plant kingdom. You can also find the oldest operating university astronomical observatory inside the gardens.

HIGHLIGHTS ALONG THE ROUTES

Route 1/Purple

(26 min walk, 1.9 km): Destination Welcome Reception in the City Hall

1. The national ethnology museum "Leiden Volkenkunde museum" and former academic hospital (built 1867).
2. Auhentic tower mill "de Valk" dating 1743
3. Museum "Lakenhal", situated in 17th century marketplace for broadcloth, now houses art from famous national and local artists, amongst others Rembrandt van Rijn, Lucas van Leyden, and Theo van Doesburg.
4. The Leiden Weigh House opened in 1659. For centuries, merchants came here to weigh and trade a variety of goods. Located at the Nieuwe Rijn it could easily be reached by boat. Now it houses a restaurant.
5. Fort of Leiden (Burcht van Leiden): old shell-keep, its origins dating back to the 11th century.
6. Leiden American Pilgrim Museum: this small museum tells the story of the founders of New-England, the Pilgrims, who fled from religious persecution in England and found refuge in Leiden before they emigrated in 1620 on the "Mayflower" to America.
7. City Hall

Route 2/Red

(25 min walk, 1.7 km): Destination Gala Dinner in Botanical Garden

8. Original Western city gate "de Morspoort", built in 1669. Of 8 city gates only 2 are still standing.
9. Typical 17th century Dutch housing: the "Kort Galgewater hof".
10. Birthplace of famous Dutch artist Rembrandt van Rijn in 1606.
11. The Sieboldhouse: unique collection of 18th-19th century Japanese objects and artifacts collected by Doctor Siebold in 1820s during his service at Deshima.
12. Dutch National Museum of Antiquities: Rich archaelogical collections of the Leiden University with artifacts from ancient Egypt, classical antiquity (Greeks, Romans, Etruscans), Ancient Near East and the Netherlands (prehistory, Roman period, and Middle Ages).
13. Hortus Botanicus: oldest botanical garden of the Netherlands, founded in 1590.
14. Academiegebouw: oldest building of the Leiden University, built in 1516.
15. Leiden Observatory: oldest university astronomical observatory in the world, established in 1633.

Congress Venue
LUMC
Hippocratespad 21

Welcome Reception
City Hall
Stadhuisplein 1
Thursday, September 22

Gala Dinner
Hortus Botanicus
Rapenburg 73
Friday, September 23

GENERAL INFORMATION

Onsite Congress Office

In case of any questions, kindly consult the ESHNR registration desk. Staff members will be happy to assist you.

Registration/Badge/Tickets

You are kindly asked to wear your badge visibly on the congress grounds at all time. Pre-ordered evening event tickets will be handed out additionally to the congress badges. Evening event tickets may be purchased onsite at the registration desk upon availability.

Certificate of Attendance

The Certificate of Attendance/CME Accreditation can be viewed and printed after the congress upon entering your ESHNR MyUserArea at the ESHNR website (www.eshnr.eu). To enter your MyUserArea, please use your lastname in combination with your personal ID printed on your congress badge.

CME Credits

Continuing Medical Education (CME) is a programme of educational activities to guarantee the maintenance and upgrading of knowledge, skills and competence following completion of postgraduate training. CME is an ethical and moral obligation for each radiologist throughout his/her professional career, in order to maintain the highest possible professional standards.

The 29th Annual Meeting and Refresher Course of ESHNR is designated up to a maximum of 17 CME credits by the European Accreditation Council for Continuing Medical Education (EACCME). Each medical specialist should only claim those hours of credit that he/she actually spent in the educational activity.

Conference Language

The meeting will be held in English; no simultaneous translation will be offered.

Onsite Registration Fees

ESHNR Member*	€ 450.00
ESHNR Non-Member	€ 585.00
Resident**	€ 330.00
Single Day Ticket***	€ 310.00

*Only available if the ESHNR 2016 membership is paid
**Requires confirmation of the institution's head by way of proof
***Only available once per person/ registration

Fee includes: Admittance to scientific sessions and exhibition, final programme including book of abstracts, refreshments and snacks during breaks, welcome reception, certificate of attendance and opening/closing ceremony.

Payment

Onsite payment can only be made by credit card (Visa or Mastercard) or in cash (Euro). Please understand that no other payment facilities like debit cards, cheques, etc. will be accepted.

Congress Venue

Leiden University Medical Center (LUMC)
Building 3
Hippocratespad 21
2333 ZD Leiden

Disclaimer/Liability

The Education Congress and Research GmbH/ESHNR cannot accept any liability for the acts of the suppliers to this meeting or the attendees' safety while travelling to or from the congress. All participants and accompanying persons are strongly advised to carry adequate travel and health insurance, as ECR GmbH/ESHNR cannot accept liability for accidents or injuries that may occur. ECR GmbH/ESHNR is not liable for personal injury and loss or damage of private property.

Name Changes

Name changes will be treated like the cancellation of the registration and a new registration of the other participant.

Mobile Phones

Please do not forget to switch off your mobile phones before entering any of the lecture rooms.

Organising Secretariat

ESHNR Office
Neutorgasse 9
1010 Vienna, Austria
Phone: +43 1 532 21 91
Fax: +43 1 532 21 91 445
office@eshnr.eu
www.eshnr.eu

Education Congress Research GmbH
Neutorgasse 9
1010 Vienna, Austria
Phone: +43 1 533 40 64
Fax: +43 1 533 40 64 448

Media Center

Speakers are reminded to check in at the Media Center at least two hours prior to their scheduled presentation. Trained staff will be available to assist you with the equipment. The Media Center should only be used for a test run of the presentation(s). Please note that the Media Center should not be used to prepare your entire presentation(s) and that due to the large number of speakers the workstations are only available for minor editing.

Opening Hours

Thursday, September 22	07:30 – 17:00
Friday, September 23	07:30 – 18:00
Saturday, September 24	07:30 – 14:30

Registration Opening Hours

Wednesday, September 21	15:00 – 17:00
Thursday, September 22	07:30 – 17:00
Friday, September 23	07:30 – 18:00
Saturday, September 24	07:30 – 15:30

Poster Exhibition – EPOS™

ESHNR 2016 is using an Electronic Presentation Online System, that offers a much greater flexibility than traditional scientific exhibits and provides better options for scientific communication.

EPOS™ Area

Several workstations are available in the Electronic Presentation Online System at which the current electronic exhibits can be viewed by the congress participants during the congress. All ESHNR electronic posters will be accessible online after the congress via the ESHNR website.

Opening Hours

Thursday, September 22	08:30 – 17:00
Friday, September 23	08:00 – 17:00
Saturday, September 24	08:00 – 15:00

NEW: Connect your own mobile device and browse through ESHNR 2016 posters:
http://cposter.ctimeetingtech.com/eshnr2016/epos

ESHNR Awards

ESHNR awards the following prizes:
€ 750.00 for the best oral presentation
€ 750.00 for the best scientific poster presentation
€ 300.00 for the best educational poster

Free registration to ESHNR 2017 – 30th Annual Meeting and Refresher Course for the second best oral presentation and second best scientific poster presentation.
Winners will be announced at the Gala Dinner on Friday, September 23, 2016.

Industry Exhibition

The industry exhibition area is located in the foyer of the ground floor.

Opening Hours

Thursday, September 22	08:30 – 17:00
Friday, September 23	08:00 – 17:00
Saturday, September 24	08:00 – 15:00

Breaks

Complimentary coffee, tea and refreshments will be served during the official coffee breaks to all congress delegates.

Future Meeting Desk

This area – located in the foyer of the ground floor – offers you an overview of future meetings in the field of radiology and related disciplines, from all over the world. Feel free to contribute flyers and posters to promote your own meetings and courses.

Guideline for Speakers

All speakers are requested to upload their presentation(s) at the ESHNR Media Center.
- You are kindly requested to submit your presentation(s) two hours before your session starts at the latest (USB sticks are recommended).
- All presentations have to be uploaded to the conference IT-system. No personal computer will be accepted for presentation.
- Please be at the lecture room at the latest five minutes prior to the start of your session and identify yourself to the moderators.
- Kindly observe exactly your presentation time. Each session contains enough time for discussion. Exceeding the time limit will not be accepted and the moderators are requested to stop presentations in such cases.

Recording

Video- or audio-recording of any sessions or presentations is not allowed without the speaker's/organiser's prior written permission.

Diploma Examination

The European Board in Head and Neck Radiology Diploma takes place on Friday, September 23, 2016. Candidates are asked to visit the staff at the registration desk beforehand.

EXHIBITION

Why visit? Source innovative products, meet new contacts and build networks!

Thursday, September 22	08:30 – 17:00
Friday, September 23	08:00 – 17:00
Saturday, September 24	08:00 – 15:00

We thank our industry partners for their highly appreciated support of ESHNR.

biomedic SAMSUNG

BRACCO LIFE FROM INSIDE

GE Healthcare

Guerbet Contrast for Life

NewTom what's next

Oldelft Benelux A CANON COMPANY

OLea MEDICAL Improved diagnosis for life™

PHILIPS

TOSHIBA

INDUSTRY SYMPOSIA

Thursday, September 22, 2016 – 11:45-13:00

Philips

New developments in CT and their impact on Head and Neck Radiology
Dr. Martin Willemink, MD, PhD

PHILIPS

Recent years have seen the emergence of a whole new range of developments in CT. Techniques such as model-based iterative reconstruction and spectral CT offer improved image quality at lower imaging dose, enhancing diagnostic capabilities of CT. This symposium will outline the characteristics of those new tools, illustrating their impact on Head and Neck Radiology with clinical cases.

Attendees of any industry symposium agree that their registration details will be forwarded to the company organising that symposium. This agreement may be cancelled at any time by writing to the ESHNR Office.

Innovation for you.
Innovation **with you.**

At Philips, we have a long history of converting research into meaningful innovation, improving the lives of clinicians and patients. We look beyond technology to the experiences of the people at the heart of care – patients, clinicians and care givers – to unlock insights across the patient journey. We are dedicated to helping you address your challenges by partnering to create meaningful innovations.

For more information see www.philips.com/healthcare

PHILIPS

LEIDEN INFORMATION

Restaurants

Leiden has hundreds of restaurants, café's and bars, serving food from all over the world. You can enjoy a culinary meal at walking distance from the venue, in one of the numerous restaurants at the Morspoort/Beestenmarkt or find a quick bite or take away meal in the Stationsstraat.

Leiden sights

Leiden, birthplace of Rembrandt and known as the Sleutelstad ("the key city") in reference to the keys in its coat of arms, is home to 120.000 people. Located at the confluence of the Old and New Rhine rivers in the province of South Holland, Leiden is a picturesque university town with many canals, almshouses and museums.

Nowadays, Leiden has one of the most highly educated populations in the Netherlands, and the university's new home for its science faculty in the Bio Science Park has helped attract high tech companies to the city and turn Leiden into a research hub.

Besides its lovingly restored centre, Leiden is also home to the Hortus Botanicus and other museums, including the Museum De Lakenhal (whose collection includes works by Rembrandt and other Dutch masters).

Between its rich history and its great academic legacy, Leiden has a stimulating mix of old and new on offer for visitors and residents alike!

NOTES

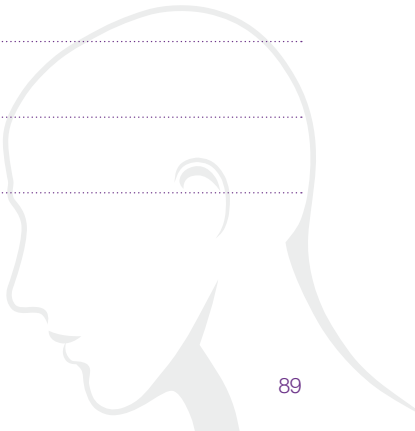

NOTES

eshnr

european society of
head and neck radiology

ESHNR 2017

30th Annual Meeting and Refresher Course

September 28–30, 2017
Lisbon/PT

www.eshnr.eu

eshnr

european society of
head and neck radiology

European Society of Head and Neck Radiology
Neutorgasse 9/2 | 1010 Vienna | Austria
phone +43 1 5322191
fax +43 1 5322191 445 | ZVR 421925549
office@eshnr.eu | www.eshnr.eu